Linear Transceiver Designs for MIMO Indoor Visible Light Communications Under Lighting Constraints

Rui Wang, *Member, IEEE*, Qian Gao, Jiayi You, Erwu Liu, *Senior Member, IEEE*, Ping Wang, Zhengyuan Xu, and Yingbo Hua, *Fellow, IEEE*

***Abstract*— In this paper, we study linear transceiver designs for indoor visible light communications (VLCs) with multiple light emitting diodes (LEDs). Specifically, we investigate VLCs including white emitting diodes and VLCs including red/green/blue (RGB) LEDs. The transmitter precoding and the offset are jointly designed by considering certain key practical lighting constraints, such as optical power, non-negativeness, and color illumination. Various non-convex transceiver design problems are formulated aiming to minimize total mean-square-error to improve transmission reliability. We show that for multi-input single-output white VLCs, the optimal precoding reduces to a simple LED selection strategy. For multi-input multi-output (MIMO) white VLCs, we prove that the optimization problem with multiple constraints can be equivalently simplified to a problem with single constraint, which enables us to propose efficient algorithms to search local optimal solutions. For MIMO RGB VLCs, by using certain useful transformations, we show that the precoding design is equivalent to covariance matrix design of transmit signals, which can be further transformed to a convex optimization problem. To develop an algorithm to find the optimal solution, we derive the optimal structure of the covariance matrix and show that the optimal solution can be obtained via a water-filling approach. Extensive simulation results are provided to verify the performance of the proposed designs.**

***Index Terms*— Visible light communication, transceiver design, convex optimization.**

Manuscript received July 21, 2016; revised December 27, 2016; accepted February 10, 2017. Date of publication February 22, 2017; date of current version June 14, 2017. This work was supported by National Key Basic Research Program of China (Grant No. 2013CB329201), Key Program of National Natural Science Foundation of China (Grant No. 61631018), National Natural Science Foundation of China (Grant No. 61401313 and 61501420), Shanghai Pujiang Program (Project No. 15PJD037), Key Research Program of Frontier Sciences of CAS (Grant No. QYZDY-SSW-JSC003), Key Project in Science and Technology of Guangdong Province (Grant No. 2014B010119001), Shenzhen Peacock Plan (No. 1108170036003286), and the Fundamental Research Funds for the Central Universities. Part of this work was presented in IEEE WCSP 2014. The correspondence author is Ping Wang. The associate editor coordinating the review of this paper and approving it for publication was H. Haas.

R. Wang, J. You, E. Liu, and P. Wang are with the Department of Information and Communications, Tongji University, Shanghai 201804, China (e-mail: ruiwang@tongji.edu.cn; 2570536004@qq.com; erwuliu@tongji.edu.cn; pwang@tongji.edu.cn).

Q. Gao is with the Key Laboratory of Wireless-Optical Communications, Chinese Academy of Sciences, School of Information Science and Technology, University of Science and Technology of China, Hefei 230026, China (e-mail: qgao@ustc.edu.cn).

Z. Xu is with the Key Laboratory of Wireless-Optical Communications, Chinese Academy of Sciences, School of Information Science and Technology, University of Science and Technology of China, Hefei 230026, China, and also with the Shenzhen Graduate School, Tsinghua University, Shenzhen 100084, China (e-mail: xuzy@ustc.edu.cn).

Y. Hua is with the Department of Electrical and Computer Engineering, University of California at Riverside, Riverside, CA 92521 USA (e-mail: yhua@ee.ucr.edu).

Color versions of one or more of the figures in this paper are available online at http://ieeexplore.ieee.org.

Digital Object Identifier 10.1109/TCOMM.2017.2672673

I. Introduction

In RECENT years, both academia and industry have shown increasing interests in the indoor visible light communications (VLCs). By taking advantage of massive deployments of light emitting diodes (LEDs), VLCs are expected to offer a potential solution to achieve a high speed wireless communication. Compared to traditional wireless radio-frequency (RF) communications, VLCs have been considered as a promising technique to alleviate the current challenges resulted by spectrum scarcity to enhance wireless transmission capacities, especially in indoor environments [2]–[5]. VLC has been standardized for wireless personal area networks (WPANs) in IEEE 802.15.7 [6] and multiple VLC transmission strategies have been proposed recently [7], [8].

In VLC systems, the signal waveforms are modulated directly as intensities which are then captured by either photodiodes (PDs) or imaging sensors at receivers. This new transmission paradigm makes the VLCs quite different from the RF communications. In particular, among the differences, the most important one is that the transmit signals in VLCs should be real and positive. Also, a good VLC system is required to be flicker-free, and satisfy specific lighting constraints such as color-rendering index (CRI) and luminous efficacy rate (LER) [5], [9]. It is noteworthy that these differences between VLCs and RF communications significantly affect the system designs of VLCs, especially in the physical layer. Despite these notable differences, advanced physical-layer techniques initially proposed for RF communications have already been modified to apply to VLCs. For example, the orthogonal frequency division multiplexing (OFDM) technique has been applied to VLC with certain non-straightforward modifications [10]–[12]. In [13]–[15], the authors studied the constellation designs for multi-carrier VLC systems by considering the power and lighting constraints with an aim to maximize the minimum distance between arbitrary two constellation symbols. In [16], the authors developed a framework for LED-based VLC systems for the transmission power and rate optimization by considering the lighting constraints.

Another advanced technique which may potentially enhance the communication capacity and improve the reliability of the VLCs is multi-input multi-output (MIMO) [15], [17]–[22]. It can be realized by deploying an array of white color LEDs or an array of red/green/blue (RGB) LEDs at the transmitter. The authors in [15] studied two limiting cases of receiver types, i.e., non-imaging and imaging MIMO systems. Corresponding channel structure and simple receiver design were also discussed in [15]. Then in [17]–[22], the MIMO transceiver is optimized to improve the system performance. Specifically, in [17], the power and the positive offset are jointly designed to improve the spectral efficiency by taking bit-error-rate requirement, nonnegativity constraint and sum optical power constraint of the transmit signals. The authors in [18] investigated a joint precoding matrix and receiving matrix design via a convergence guaranteed iterative algorithm by considering the positive constraint on the transmit signals into account. In [19]–[22], a multi-user downlink channel was considered and the corresponding precoding design were optimized. Particularly, in [19]–[21], the authors imposed the zero-forcing structure on the precoding matrix. In [22], the authors considered a two-user broadcast downlink channel and assumed that single data stream was desired by each receiver. In this case, the optimal beamformers in [22] can be obtained via a relaxed semidefinite programming problem.

In this paper, we study transceiver design for VLCs with an array of white color LEDs or an array of RGB color LEDs. The transmit precoding and the offset are jointly designed with an aim to minimize the total mean square-error (MSE) by taking certain key practical lighting constraints like optical power and non-negativeness constraints into account. In particular, the color illumination constraint is further considered for RGB color VLC system. It is noteworthy that since we consider a multiple-data-stream transmission, the joint design problems considered in our work are in general more complex than the single-data-stream transmission in [19]–[22]. Unlike [18], we consider more practical lighting constraints which make our design more challenging. Furthermore, unlike [17] and [19]–[21], our designs include the case where no suboptimal structure is assumed for the transmit precoding matrix. The main contributions of this work are summarized as follows.

- Different non-convex transceiver design problems are formulated aiming to minimize the total MSE;
- We show that for MISO white color VLCs, the optimal precoding reduces to a simple LED selection strategy;
- For the MIMO white color VLC, we prove that the optimization problem with multiple constraints can be equivalently simplified to a problem with single constraint, which enables us to develop efficient algorithms to search local optimal solutions;
- For the MIMO RGB VLCs, by using certain useful transformations, we show that the precoding design is equivalent to the covariance matrix design of transmit signals, which can be further transformed to a convex optimization problem. To find optimal solution, we derive the optimal structure of the covariance matrix and show that the optimal solution can be obtained via water-filling approach.

The rest of the paper is organized as follows. In Section II, we present the system model. The joint precoding and offset desgin for the MIMO white color VLC is considered in Section III. The joint precoding and offset desgin for the MIMO RGB color VLC is considered in Section IV. Simulation results are provided in Section V. Finally, we conclude the paper in Section VI.

Notations: $\mathbb{E}(\cdot)$ denotes the expectation operator. Superscripts $\mathbf{A}^T$, $\mathbf{A}^*$, and $\mathbf{A}^H$ denote the transpose, conjugate, and conjugate transpose of matrix $\mathbf{A}$, respectively. $\mathrm{Tr}(\mathbf{A})$, $\mathbf{A}^{-1}$, $\det(\mathbf{A})$, and $\mathrm{Rank}(\mathbf{A})$ stand for the trace, inverse, determinant, and rank of $\mathbf{A}$, respectively. $\mathrm{Diag}(\mathbf{a})$ denotes a diagonal matrix with $\mathbf{a}$ being its diagonal entries. $\mathbf{0}$ and $\mathbf{I}$ denote the zero and identity matrices, respectively. The distribution of a circular symmetric complex Gaussian vector with mean vector $\mathbf{x}$ and covariance matrix Σ is denoted by $\mathcal{C}N(\mathbf{x}, \Sigma)$. $\mathbb{R}^{x\times y}$ denotes the space of real $x \times y$ matrices. $\mathbf{A} \succeq \mathbf{0}$ implies that matrix $\mathbf{A}$ is a semidefinite positive matrix. $||\cdot||_l$ denotes l-norm. $\mathrm{abs}(\cdot)$ denotes the absolute value.

II. System Model

In this section, we present the channel models of the MIMO white VLC system and the MIMO RGB VLC system. The corresponding joint precoding and offset optimization problems are also formulated. The design solutions of two VLC systems are presented in Section IV and Section III, respectively. We will observe that the design for the RGB VLC system is more challenging than the one for the white VLC system, as we need to put a special color illumination constraint on the power allocation among the red, green, and blue color bands to avoid color shift.

A. MIMO White VLC

Consider an optical wireless MIMO system with N_t transmit LEDs and N_r receive PDs. The received signal at the receiver $\mathbf{y} = [y_1, y_2, \cdots, y_{N_r}]$ can be written as

$$\mathbf{y} = \mathbf{H}\mathbf{x} + \mathbf{n}, \tag{1}$$

where $\mathbf{H} \in \mathbb{R}^{N_r\times N_t}$ denotes the channel matrix, $\mathbf{n}$ denotes the narrow-band additive Gaussian noise (AWGN) following the distribution of $\mathcal{N}(\mathbf{0}, \sigma^2\mathbf{I})$. The transmitted signal $\mathbf{x} = [x_1, x_2, \cdots, x_{N_t}]$ can be represented as

$$\mathbf{x} = \mathbf{F}\mathbf{d} + \mathbf{b}, \tag{2}$$

where $\mathbf{d} = [d_1, d_2, \cdots, d_N]$ with N being the number of the transmit data streams is the output vector of a multi-level pulse amplitude modulation (PAM) with zero mean, i.e., $\mathbb{E}(\mathbf{d}) = \mathbf{0}$; $\mathbf{b}$ is a positive real offset vector to guarantee the non-negativeness of the resulting intensity vector used to modulate the lights, i.e., $\mathbf{x} \geq \mathbf{0}$. In addition, the constellation of multi-level PAM is formed in the range of $[-\triangle, \triangle]$, where $2\triangle$ is the maximum possible distance between two constellation points. We assume that d_i is taken from one of a M-PAM symbol with $M = 2^k$ and k is the number of bits per symbol.

$\mathbf{F} \in \mathcal{R}^{N_t \times N}$ is the precoding matrix. With (2), the received signal at the receiver can be represented as

$$\mathbf{y} = \mathbf{HFd} + \mathbf{Hb} + \mathbf{n}. \tag{3}$$

At the receiver side, the term $\mathbf{Hb}$ is subtracted from $\mathbf{y}$ before the equalization. After this subtraction, the communication model can be written as

$$\tilde{\mathbf{y}} = \mathbf{HFd} + \mathbf{n}. \tag{4}$$

Here, we assume that the linear minimum mean-square-error (MMSE) equalizer $\mathbf{W}$ is used. The estimated symbols by the MMSE equalizer can be expressed as follows

$$\hat{\mathbf{d}} = \mathbf{W}(\mathbf{y} - \mathbf{Hb}) = \mathbf{W}(\mathbf{HFd} + \mathbf{n}). \tag{5}$$

Assume $\mathbb{E}(\mathbf{dd}^T) = \mathbf{D} = \text{Diag}([D, D, \cdots, D])$ with $D = \frac{\triangle^2(M+1)}{3(M-1)}$, The optimal $\mathbf{W}$ is

$$\mathbf{W} = \mathbf{DF}^T\mathbf{H}^T\left(\mathbf{HFDF}^T\mathbf{H}^T + \sigma^2\mathbf{I}\right)^{-1}. \tag{6}$$

The associated mean-square-error covariance matrix can be written as

$$\mathbf{R} = \mathbb{E}\left[(\mathbf{d} - \hat{\mathbf{d}})(\mathbf{d} - \hat{\mathbf{d}})^T\right] = \left(\mathbf{D}^{-1} + \frac{1}{\sigma^2}\mathbf{F}^T\mathbf{H}^T\mathbf{HF}\right)^{-1}. \tag{7}$$

Now we discuss the power constraint for VLC communication systems. Each element of the transmit signal vector $\mathbf{x}$ is already a power value in the context of VLC. The averaged power of $\mathbf{x}$ is hence given by

$$\mathbb{E}(\mathbf{x}) = \mathbb{E}(\mathbf{Fd} + \mathbf{b}) = \mathbf{b}. \tag{8}$$

Let P be the total averaged transmission power. We set the power constraint for our designs as

$$\mathbf{1}^T\mathbf{b} \leq P. \tag{9}$$

Therefore, the overall optimization problem can be formulated as

$$\begin{aligned} \min_{\mathbf{F},\mathbf{b}} \ & \text{Tr}\left[\left(\mathbf{D}^{-1} + \frac{1}{\sigma^2}\mathbf{F}^T\mathbf{H}^T\mathbf{HF}\right)^{-1}\right] \\ \text{s.t. } & \mathbf{1}^T\mathbf{b} \leq P \\ & \mathbf{b} \geq \mathbf{0} \\ & \mathbf{Fd} + \mathbf{b} \geq \mathbf{0} | \mathbf{d}, \quad \forall \mathbf{d} \end{aligned} \tag{10}$$

B. MIMO RGB VLC

We consider a VLC system employing RGB LEDs to transmit information. To be specific, in each color band, we use N_t LEDs to transmit and use N_r PDs to receive. In this case, if the elements in $\mathbf{y}$ are sorted by $\mathbf{y} = [\mathbf{y}_r^T, \mathbf{y}_g^T, \mathbf{y}_b^T]^T$, the received signal can be rewritten explicitly as

$$\mathbf{y} = \begin{bmatrix} \mathbf{y}_r \\ \mathbf{y}_g \\ \mathbf{y}_b \end{bmatrix} = \mathbf{H}_{rgb}\begin{bmatrix} \mathbf{x}_r \\ \mathbf{x}_g \\ \mathbf{x}_b \end{bmatrix} + \begin{bmatrix} \mathbf{n}_r \\ \mathbf{n}_g \\ \mathbf{n}_b \end{bmatrix}, \tag{11}$$

where $\mathbf{H}_{rgb} \in \mathbb{R}^{3N_r \times 3N_t}$, $\mathbf{n}_i$, $i = r, g, b$, is addtive AWGN following $\mathcal{N}(\mathbf{0}, \sigma^2\mathbf{I}_{N_r})$. The detailed structure of $\mathbf{H}_{rgb}$ will be given in Subsection V-A.

In (11), we denote the transmit signal $\mathbf{x}$ as $\mathbf{x} = [\mathbf{x}_r^T, \mathbf{x}_g^T, \mathbf{x}_b^T]^T$, which can also be represented as in (2) and the corresponding $\mathbf{d}$ and $\mathbf{b}$ have forms of $\mathbf{d} = [\mathbf{d}_r^T, \mathbf{d}_g^T, \mathbf{d}_b^T]^T$ and $\mathbf{b} = [\mathbf{b}_r^T, \mathbf{b}_g^T, \mathbf{b}_b^T]^T$, respectively. Similarly to the white color case, the non-negative constraint requires $\mathbf{Fd} + \mathbf{b} \geq \mathbf{0}$. For the power constraint, we consider both the total average power across all LEDS and the color illumination requirements. Denote the average optical power across all LEDs over a long time as P and the average power splitting vector as $\bar{\mathbf{x}} = [\bar{x}_r, \bar{x}_g, \bar{x}_b]$, where $\bar{x}_i > 0$, $i = r, g, b$, and $\bar{x}_r + \bar{x}_g + \bar{x}_b = 1$. Here we assume that $\bar{x_r}$, $\bar{x_g}$, and $\bar{x_b}$ are fixed and determined by the illumination scheme, and color shift is avoided when a proper illumination scheme is selected. The physical meaning of element $\bar{x}_i$, $i = \{r, g, b\}$, can be considered as the percentage of the total power we assign to the signals modulated on color band i. We can thus write the optical power and the color illumination requirements into a single constraint since the following relation holds

$$\mathbb{E}\big[\mathbf{J}(\mathbf{Fd} + \mathbf{b})\big] = \mathbf{JF}\mathbb{E}[\mathbf{d}] + \mathbf{Jb} = \mathbf{Jb} = P\bar{\mathbf{x}}, \tag{12}$$

where by definition $\mathbb{E}(\mathbf{d}) = \mathbf{0}$ and $\mathbf{J}$ is a $3 \times 3N_t$ selection matrix in a form of

$$\mathbf{J} = \begin{bmatrix} \mathbf{1}_{1\times N_t} & \mathbf{0}_{1\times N_t} & \mathbf{0}_{1\times N_t} \\ \mathbf{0}_{1\times N_t} & \mathbf{1}_{1\times N_t} & \mathbf{0}_{1\times N_t} \\ \mathbf{0}_{1\times N_t} & \mathbf{0}_{1\times N_t} & \mathbf{1}_{1\times N_t} \end{bmatrix}. \tag{13}$$

The inner product between each row of $\mathbf{J}$ and the vector $\mathbf{b}$ sums up the intensities of the corresponding colored LEDs. Then, the overall optimization problem for the multiple color case can be summarized as

$$\begin{aligned} \min_{\mathbf{F},\mathbf{b}} \ & \text{Tr}\left[\left(\mathbf{D}^{-1} + \frac{1}{\sigma^2}\mathbf{F}^T\mathbf{H}^T\mathbf{HF}\right)^{-1}\right] \\ \text{s.t. } & \mathbf{b} \geq \mathbf{0} \\ & \mathbf{Fd} + \mathbf{b} \geq \mathbf{0} | \mathbf{d}, \forall \mathbf{d} \\ & \mathbf{Jb} = P\bar{\mathbf{x}} \end{aligned} \tag{14}$$

C. Channel Sate Information (CSI) Acquirement and Impact of Imperfect CSI

In practical VLC systems, we assume that the channel is estimated at the receiver by letting the transmitter send a pilot known by the receiver. Then, the receiver feeds back the estimated CSI to the transmitter. As compared to the wireless communications, the channel in the VLC system changes slowly. The feedback of the CSI from receiver to the transmitter is not required to be updated very often.

It is noticed that in design problems (10) and (14), we assume that the CSI is perfectly known. In practice, CSI uncertainty is inherent in VLC systems due to the imperfect channel estimation and capacity limitation of the feedback links. With CSI errors, the designs we proposed in the following sections cannot be directly used. In general, we need to include the CSI errors in the design optimization problems (10) and (14) based the type of errors, i.e., bounded by a norm set [32] or known with the statistical information [18]. Considering the CSI errors will make the designs more challenging. We admit

that the joint design of beamforming and offset with channel errors is an interesting research topic, but this is out of the scope of this paper.

Before leaving this section, we provide some discussions on the illumination issue of the precoding designs. Our designs in (10) and (14) aim to improve the performance of data transmission. Here we implicitly assume that the illumination requirement is satisfied. In fact, we assume that the DC bias is composed of two parts: the fixed part which is to guarantee that the transmit LEDs are turned on and an adaptive part as is optimized by our designs mainly for communications purpose (i.e., the power P in (10) and (14)).

III. Joint Precoding and Offset Design for the MIMO White VLC Systems

In this section, we present how to perform the joint precoding and offset design for the MIMO white VLC system. In particular, we show that the joint design reduces to a simple LED selection scheme for the MISO white VLC system.

A. MIMO White VLC System

As noted before, the joint optimization problem in (10) depends on specific transmit symbols in $\mathbf{d}$. To enable our design for arbitrary symbols, we in general need to try all possible combinations of symbols, which will largely complicate the joint design. However, here we actually only need to consider the worst case where we require that the smallest value in $\mathbf{Fd}+\mathbf{b}$ is not less than zero. That is, the constraint $\mathbf{Fd}+\mathbf{b} \geq \mathbf{0}|\mathbf{d}, \forall \mathbf{d}$ is equivalent to $\mathbf{b}-\text{abs}(\mathbf{F})\mathbf{\Delta} \geq \mathbf{0}$ with $\mathbf{\Delta}=[\Delta, \Delta, \cdots, \Delta]^T$. This changes (10) to

$$\min_{\mathbf{F},\mathbf{b}} \ \text{Tr}\left[\left(\mathbf{D}^{-1}+\frac{1}{\sigma^2}\mathbf{F}^T\mathbf{H}^T\mathbf{H}\mathbf{F}\right)^{-1}\right] \tag{15a}$$

$$\text{s.t. } \mathbf{1}^T\mathbf{b} \leq P \tag{15b}$$

$$\mathbf{b} \geq \mathbf{0} \tag{15c}$$

$$\mathbf{b}-\text{abs}(\mathbf{F})\mathbf{\Delta} \geq \mathbf{0} \tag{15d}$$

Lemma 1: The optimization problem (15) *is nonconvex with respect to variables* $\mathbf{F}$ *and* $\mathbf{b}$.

Proof: Please refer to Appendix A. □

Due to the nonconvexity of (15), we propose two methods in what follows to find the solution. Before that, we present some properties of problem (15), which is helpful to simplify the original design problem.

Lemma 2: In (15)*, the optimal solution must satisfy* $\mathbf{b}-\text{abs}(\mathbf{F})\mathbf{\Delta}=\mathbf{0}$.

Proof: Denote by $\mathbf{f}_i$ the i-th row of $\mathbf{F}$. If at the optimal solution, we have $b_n-\text{abs}(\mathbf{f}_n) > 0$ where $n \in \mathcal{S}$ with $\mathcal{S} \subseteq \{1, 2, \cdots, N\}$. Then we can always extract some power from b_n with $n \in \mathcal{S}$, and allocate this power to b_n with $n \in \bar{\mathcal{S}}$ with $\bar{\mathcal{S}}=\{1, 2, \cdots, N\}\backslash\mathcal{S}$. In this case, we update b_n and $\mathbf{F}$ as $\tilde{b}_n$ and $\tilde{\mathbf{F}}=\alpha\mathbf{F}$ where $\alpha \geq 1$ is a positive value such that $\tilde{\mathbf{b}}-\text{abs}(\tilde{\mathbf{F}})\mathbf{\Delta}=\mathbf{0}$. $\tilde{\mathbf{F}}$ can be utilized to decrease the value of objective, which contradicts the optimality assumption made before. Lemma 2 is thus proven. □

Based on Lemma 2, the optimization problem (15) becomes

$$\begin{aligned}\min_{\mathbf{F},\mathbf{b}} \ &\text{Tr}\left[\left(\mathbf{D}^{-1}+\frac{1}{\sigma^2}\mathbf{F}^T\mathbf{H}^T\mathbf{H}\mathbf{F}\right)^{-1}\right]\\ \text{s.t. } &\mathbf{1}^T\mathbf{b} \leq P\\ &\mathbf{b} \geq \mathbf{0}\\ &\mathbf{b}=\text{abs}(\mathbf{F})\mathbf{\Delta}\end{aligned} \tag{16}$$

which is equivalent to

$$\begin{aligned}\min_{\mathbf{F},\mathbf{b}} \ &\text{Tr}\left[\left(\mathbf{D}^{-1}+\frac{1}{\sigma^2}\mathbf{F}^T\mathbf{H}^T\mathbf{H}\mathbf{F}\right)^{-1}\right]\\ \text{s.t. } &\mathbf{1}^T\text{abs}(\mathbf{F})\mathbf{\Delta} \leq P.\end{aligned} \tag{17}$$

Lemma 3: In (17)*, the optimal solution must satisfy* $\mathbf{1}^T\text{abs}(\mathbf{F})\mathbf{\Delta}=P$.

Proof: If the optimal $\mathbf{F}$ does not activate the constraint in (17), we can always update $\mathbf{F}$ as $\beta\mathbf{F}$ with $\beta \geq 1$ to activate the constraint in (17) and reduce the value of the objective function. This contradicts with the optimality assumption. □

Based on Lemma 2 and Lemma 3, the optimization problem (17) is equivalent to

$$\begin{aligned}\min_{\mathbf{F}} \ &\text{Tr}\left[\left(c\mathbf{I}+\mathbf{F}^T\mathbf{H}^T\mathbf{H}\mathbf{F}\right)^{-1}\right]\\ \text{s.t. } &\mathbf{1}^T\text{abs}(\mathbf{F})\mathbf{1}=\frac{P}{\Delta}\end{aligned} \tag{18}$$

where $c=\frac{\sigma^2}{D}$. After solving (18), the optimal $\mathbf{b}$ is obtained by $\mathbf{b}=\text{abs}(\mathbf{F})\mathbf{\Delta}$.

Unlike the problem in RF communications [23], we have a different power constraint here, which makes our problem more challenging. In what follows, we propose two methods to solve (18).

1) SVD Based Precoding Design: For point-to-point RF communications, it has been proven in [23] that the optimal structure of user precoding matrix can be determined by performing the single value decomposition (SVD) on the channel matrix. Here we borrow this idea by assuming that the precoding matrix $\mathbf{F}$ has certain structure, which will simplify the design problem (18). Denote SVD of channel matrix $\mathbf{H}$ as $\mathbf{H}=\mathbf{U}_H\mathbf{D}_H\mathbf{V}_H^T$, where $\mathbf{D}_H=\text{Diag}\left([d_{H,1}, d_{H,2}, \cdots, d_{H,M}]\right)$ with $M=\min(N_t, N_r)$, and $\mathbf{U}_H$ and $\mathbf{V}_H$ are two real unitary matrices. In SVD based precoding, the total number of transmitted data streams is N with $N \leq M$. Further, we assume that the source precoder has a structure of

$$\mathbf{F}=\bar{\mathbf{V}}_H\mathbf{D}_F, \tag{19}$$

where $\mathbf{D}_F=\text{Diag}([d_{F,1}, d_{F,2}, \cdots, d_{F,N}])$ and the columns of $\bar{\mathbf{V}}_H$ correspond to N columns of $\mathbf{V}^T$ with N largest eigenvalues. Although the SVD based structure is optimal for RF communication systems, it is not necessarily optimal in VLC system as they have completely different system setups. However, here we apply this structure as it has a clear physical meaning, that is, it parallelizes the MIMO channel into a set of parallel non-interference channels.

Using the precoder structure given in (19), the optimization problem (18) reduces to[1]

$$\min_{d_{F,i},\forall i} \sum_{i=1}^{N} \frac{1}{c + d_{H,i}^2 d_{F,i}^2}$$
$$\text{s.t.} \sum_{i=1}^{N} |d_{F,i}| a_i \le \frac{P}{\Delta} \tag{20}$$

where $a_i = ||\mathbf{v}_{H,i}||_1$ with $\mathbf{v}_{H,i}$ being the i-th column of $\bar{\mathbf{V}}_H$. Note that in (20), the sign of $d_{F,i}$ does not affect either the value of the objective function nor the constraints. Without loss of generality, we assume $d_{F,i} \ge 0$ for all i. Then (20) reduces to

$$\min_{d_{F,i}\ge 0} \sum_{i=1}^{N} \frac{1}{c + d_{H,i}^2 d_{F,i}^2}$$
$$\text{s.t.} \sum_{i=1}^{N} d_{F,i} a_i \le \frac{P}{\Delta}. \tag{21}$$

It can be observed that (21) is nonconvex as the objective function is a nonconvex function. However, we can readily prove that the objective function is monotonic. Moreover, the feasible set constructed by the power constraint is a normal set [27]. We thus conclude that the optimal solution of (21) must be on the boundary of the feasible set. Based on this fact, the optimal solution of (21) can be asymptotically found in finite round of iterations with the technique of the monotonic optimization [29], where the main idea is to iteratively use the polyblock approximation to find a tight outbound of the feasible set, then to get the approximate optimal solution. In monotonic optimization, we first need to find a box $[\mathbf{0}, \mathbf{c}]$ to enclose the feasible set of (21). Here $\mathbf{c}$ can be chosen as $\mathbf{c} = [\frac{P}{\Delta}, \frac{P}{\Delta}, \cdots, \frac{P}{\Delta}]$. The second key step in monotonic optimization is to find the projection of $\mathbf{z}$ outside of the feasible set on the boundary of the feasible set, denoted by $\pi_{\mathcal{G}}(\mathbf{z})$, where $\mathcal{G}$ denotes the feasible set. Note that as the feasible set constructed by the power constraint is actually a simplex, the projection $\pi_{\mathcal{G}}(\mathbf{z})$ reduces to find a scalar δ to update $\mathbf{z}$ as $\delta\mathbf{z}$ such that $\sum_{i=1}^{N} \delta a_i z_i = \frac{P}{\Delta}$. δ can be determined as

$$\delta = \frac{P/\Delta}{\sum_{i=1}^{N} a_i z_i}. \tag{22}$$

Further, to make the iterations converge, as shown in [29], we need to optimize the modified problem with a shift of origin given as

$$\min_{d_{F,i}\ge 1} \sum_{i=1}^{N} \frac{1}{c + (d_{H,i}-1)^2 d_{F,i}^2}$$
$$\text{s.t.} \sum_{i=1}^{N} (d_{F,i}-1) a_i \le \frac{P}{\Delta}. \tag{23}$$

Denote the feasible set in (23) by $\mathcal{G}$, and specify the objective function as $f(\mathbf{d}_F)$ with $\mathbf{d}_F = [d_{F,1}, d_{F,2}, \cdots, d_{F,N}]^T$. Furthermore, the value of the objective function in the k-th iteration is denoted as $\text{MSE}^{[k]}$, where index $[k]$ denotes the number of iteration. The overall algorithm based on monotonic optimization [29] is summarized in Algorithm 1.

Algorithm 1

- **Initialization** Let the initial polyblock be box $[\mathbf{0}, \mathbf{b}]$ that encloses $\mathcal{G}$. The vertex set $\mathcal{T}^{[0]} = \{\mathbf{b}\}$. Let $\epsilon \ge 0$ be a small positive value and set $\text{MSE}^{[0]} = -\infty$ and iteration number k as $k = 0$.
- **Repeat**
  - $k = k + 1$
  - From vertex set $\mathcal{T}^{[k]}$, find $\mathbf{z}^{[k]} \in \text{argmin}\{f(\mathbf{z}) | \mathbf{z} \in \mathcal{T}^{[k]}\}$.
  - Compute $\pi_{\mathcal{G}}(\mathbf{z}^{[k]})$, the projection of $\mathbf{z}^{[k]}$ on the upper boundary of $\mathcal{G}$.
  - **if** $\pi_{\mathcal{G}}(\mathbf{z}^{[k]}) = \mathbf{z}^{[k]}$
  - Set the current best solution $\bar{\mathbf{x}}^{[k]}$ as $\bar{\mathbf{x}}^{[k]} = \mathbf{z}^{[k]}$ and $\text{MSE}^{[k]} = f(\mathbf{z}^{[k]})$.
  - **else**
  - If $\pi_{\mathcal{G}}(\mathbf{z}^{[k]}) \in \mathcal{G}$ and $f(\pi_{\mathcal{G}}(\mathbf{z}^{[k]})) \le \text{MSE}^{[k-1]}$, let the current best solution $\bar{\mathbf{x}}^{[k]} = \pi_{\mathcal{G}}(\mathbf{z}^{[k]})$. Otherwise, $\bar{\mathbf{x}}^{[k]} = \bar{\mathbf{x}}^{[k-1]}$ and $\text{MSE}^{[k]} = \text{MSE}^{[k-1]}$.
  - Let $\mathbf{x} = \pi_{\mathcal{G}}(\mathbf{z}^{[k]})$ and $\mathcal{T}^{[k+1]} = (\mathcal{T}^{[k]} \backslash \mathcal{T}_*) \cup \{\mathbf{v}^i = \mathbf{v} + (x_i - v_i)\mathbf{e}^i | \mathbf{v} \in \mathcal{T}_*, i \in \{1, \cdots, n\}\}$, where $\mathcal{T}_* = \{\mathbf{v} \in \mathcal{T}_k | \mathbf{v} > \mathbf{x}\}$.
  - Remove from $\mathcal{T}_{k+1}$ improper vertices.
  - **end if**
- **Until** $\mathcal{T}_{k+1} = \emptyset$
- Let $\mathbf{x}^* = \bar{\mathbf{x}}_k$ and terminate the algorithm.

2) Subgradient Based Precoding Design: In the proposed SVD based precoding design, we assume that the source precoder has a specific structure so that the effective channel becomes a set of parallel channels without inter-stream interference. This structure is not necessarily optimal here due to the different power constraint from the RF communications. In this subsection, we give a new precoding design algorithm in which we do not impose any given precoder structure on $\mathbf{F}$. Specifically, we directly optimize the precoding matrix $\mathbf{F}$. We rewrite the optimization problem (18) as

$$\min_{\mathbf{F}} \; f(\mathbf{F}) = \text{Tr}\left[\left(c\mathbf{I} + \mathbf{F}^T\mathbf{H}^T\mathbf{H}\mathbf{F}\right)^{-1}\right]$$
$$\text{s.t.} \; ||\mathbf{F}||_1 \le \frac{P}{\Delta}. \tag{24}$$

The equal constraint in problem (18) can be replaced by the unequal one in (24) as the optimal value of (24) must activate the 1-norm constraint. Here the change from (18) to (24) enlarges the feasible region, which will facilitate us to develop the following gradient based algorithm.

To deal with the optimization in (24), we next develop a gradient projection (GP) algorithm. GP algorithm is a generalization of the unconstrained steepest descent algorithm, and in general converges faster then the conditional gradient method. As the considered optimization is nonconvex, the GP algorithm can only converge to a local suboptimal solution,

[1]It is noted that to reduce the precoder design in (18) to the power allocation problem in (20), the range parameters D for different data streams should keep the same.

the gap to the optimal solution depends on the choice of the initial point. The general form of the GP algorithm is given as follows

$$\mathbf{F}^{[k+1]} = \mathbf{F}^{[k]} + \alpha^{[k]}(\bar{\mathbf{F}}^{[k]} - \mathbf{F}^{[k]}), \tag{25}$$

where $\mathbf{F}^{[k]}$ is the updated precoding matrix in the k-th iteration, $\alpha^{[k]} \in (0, 1]$ is the step size used in the k-th iteration, and $\bar{\mathbf{F}}^{[k]}$ is given by

$$\bar{\mathbf{F}}^{[k]} = \text{proj}\left[\mathbf{F}^{[k]} - s^{[k]}\nabla f(\mathbf{F}^{[k]})\right], \tag{26}$$

where proj$[\cdot]$ denotes the projection onto the feasible set of (24), and $s^{[k]}$ is a positive scalar. In (26), to obtain $\bar{\mathbf{F}}^{[k]}$, we take a step $-s^{[k]}\nabla f(\mathbf{F}^{[k]})$ along the steepest descent, and then project $\mathbf{F}^{[k]} - s^{[k]}\nabla f(\mathbf{F}^{[k]})$ onto the feasible set region of (24), thereby obtaining the feasible matrix $\bar{\mathbf{F}}^{[k]}$. Note that as (25) can be rewritten by

$$\mathbf{F}^{[k+1]} = \alpha^{[k]}\bar{\mathbf{F}}^{[k]} + (1 - \alpha^{[k]})\mathbf{F}^{[k]}, \tag{27}$$

we obtain that $\mathbf{F}^{[k+1]}$ is always in the feasible region of (24) due to the fact that the 1-norm constraint in (24) is convex. Now the key steps in (25) and (26) are to derive the gradient $\nabla f(\mathbf{F})$ and to conduct the projection proj$[\cdot]$ in (26). Using the rules of $\partial \text{Tr}(\mathbf{X}^{-1}\mathbf{A}) = -\text{Tr}(\mathbf{X}^{-1}\partial\mathbf{X}\mathbf{X}^{-1}\mathbf{A})$, we have

$$\nabla f(\mathbf{F}) = -2\mathbf{H}^T\mathbf{H}\mathbf{F}\left(c\mathbf{I} + \mathbf{F}^T\mathbf{H}^T\mathbf{H}\mathbf{F}\right)^{-2}. \tag{28}$$

$s^{[k]}$ and $\alpha^{[k]}$ in (25) and (26) are scalars of the step size and can be chosen according to the Armijo rule [28]. In this rule, $s^{[k]} = s$ is a constant throughout the iterations, and $\alpha^{[k]} = \theta^{m_k}$, where m_k is the minimal nonnegative integer that satisfies the following inequality

$$f(\mathbf{F}^{[k+1]}) - f(\mathbf{F}^{[k]}) \leq \sigma\theta^{m_k}\text{Tr}\left[\nabla f(\mathbf{F}^{[k]})^T\left(\bar{\mathbf{F}}^{[k]} - \mathbf{F}^{[k]}\right)\right], \tag{29}$$

where σ and θ are constants, and σ is a parameter close to 0, and θ a proper choice from 0.1 to 0.5 [28]. Now we consider the projection process. Denote by $\mathcal{G}$ the convex feasible region constructed by the constraint $||\mathbf{F}||_1 \leq \frac{P}{\Delta}$. The projection is actually equivalent to the following optimization problem

$$\begin{aligned} &\min_{\mathbf{X}} \ g(\mathbf{X}) = ||\mathbf{Z} - \mathbf{X}||_F^2 \\ &\text{s.t. } \mathbf{X} \in \mathcal{G} \end{aligned} \tag{30}$$

where we assume $\mathbf{Z} = \mathbf{F}^{[k]} - s^{[k]}\nabla f(\mathbf{F}^{[k]})$. Note that as the objective function in (30) is convex, the optimal solution in (30) can be efficiently found via interior point algorithm etc. In addition, when $\mathbf{Z} \in \mathcal{G}$, the optimal solution of $\mathbf{X}$ in (30) reduces to $\mathbf{X} = \mathbf{Z}$. For the nontrivial case, we try to solve (30) by solving its dual problem, which will be shown to have less complexity. Denote by λ the lagrangian coefficient associated with the power constraint in (30) satisfying $\lambda \geq 0$. The lagrangian function can be denoted by

$$\mathcal{L} = ||\mathbf{z} - \mathbf{x}||_2^2 + \lambda(||\mathbf{x}||_1 - \frac{P}{\Delta}), \tag{31}$$

where $\mathbf{z} = \text{vec}(\mathbf{Z})$ and $\mathbf{x} = \text{vec}(\mathbf{X})$. The Lagrange dual function of (30) is readily obtained as

$$\begin{aligned} g(\lambda) &= \inf_{\mathbf{x}} \mathcal{L} = \inf_{\mathbf{x}} \left(||\mathbf{z} - \mathbf{x}||_2^2 + \lambda(||\mathbf{x}||_1 - \frac{P}{\Delta})\right) \\ &= \inf_{\mathbf{x}} \left(\sum_{k=1}^{NN_t}(z_k - x_k)^2 + \lambda|x_k| - \lambda\frac{P}{\Delta}\right). \end{aligned} \tag{32}$$

For convenience, we define

$$g_k(\lambda) = \inf_{x_k}(z_k - x_k)^2 + \lambda|x_k|. \tag{33}$$

The solution of (33) is given as

$$x_k^* = \begin{cases} z_k + \frac{1}{2}\lambda & z_k \leq -\frac{1}{2}\lambda \\ 0 & |z_k| < \frac{1}{2}\lambda \\ z_k - \frac{1}{2}\lambda & z_k \geq \frac{1}{2}\lambda, \end{cases} \tag{34}$$

which implies that

$$g_k(\lambda) = \begin{cases} -(\frac{1}{2}\lambda - |z_k|)^2 + z_k^2 & \lambda \leq 2|z_k| \\ z_k^2 & \lambda > 2|z_k|. \end{cases} \tag{35}$$

The dual problem of (30) can thus be written as

$$\begin{aligned} &\max_{\lambda} \ g(\lambda) = \sum_k g_k(\lambda) - \lambda\frac{P}{\Delta} \\ &\text{s.t. } \lambda \geq 0 \end{aligned} \tag{36}$$

which is a concave optimization problem. To obtain the solution, we first have

$$g_k'(\lambda) = \begin{cases} |z_k| - \frac{1}{2}\lambda & \lambda \leq 2|z_k| \\ 0 & \lambda \geq 2|z_k|. \end{cases} \tag{37}$$

If $||\mathbf{z}||_1 > \frac{P}{\Delta}$, the optimal λ is obtained as

$$\lambda^* = \max(0, \bar{\lambda}), \tag{38}$$

where $\bar{\lambda}$ denotes the roof of the function of

$$g'(\lambda) = \sum_k \max(|z_k| - \frac{1}{2}\lambda, 0) - \frac{P}{\Delta}. \tag{39}$$

Sort the values of $\{|z_1|, |z_2|, \cdots, |z_{NN_t}|\}$ as $\{|z_{[1]}|, |z_{[2]}|, \cdots, |z_{[NN_t]}|\}$ and $z_{[0]} \leq |z_{[1]}| \leq |z_{[2]}| \leq \cdots \leq |z_{[NN_t]}|$ with $z_{[0]} = 0$, it is easy to verify that if $\lambda^* \neq 0$, λ^* must be in the interval of $2z_{[i]}$ and $2z_{[i+1]}$ where index i makes $g'(2|z_{[i]}|) \geq 0$ and $g'(|2z_{[i+1]}|) \leq 0$. After determining i, we have

$$\lambda^* = \frac{2\left(\sum_{k=i+1}^{NN_t}|z_{[k]}| - \frac{P}{\Delta}\right)}{NN_t - i}. \tag{40}$$

B. MISO White VLC System

In this subsection, we consider a special case of the MIMO white VLC systems where only the transmitter is equipped with multiple LEDs, i.e., MISO white VLC system. In this case, we assume that only one data stream is transmitted from multiple transmit LEDs to achieve diversity gain. The performance of the MISO VLC system is evaluated by the

signal noise ratio (SNR) defined as $\text{SNR} = \frac{|\mathbf{f}^T\mathbf{h}|^2}{\sigma^2}$. The precoding design problem in (15) reduces to

$$\begin{aligned} \max_{\mathbf{f},\mathbf{b}} \ & \frac{|\mathbf{f}^T\mathbf{h}|^2}{\sigma^2} \\ \text{s.t. } & \mathbf{1}^T\mathbf{b} \le P \\ & \mathbf{b} \ge \mathbf{0} \\ & \mathbf{b} - \text{abs}(\mathbf{f})\Delta \ge \mathbf{0}. \end{aligned} \tag{41}$$

By taking a closer look at (41), we can find that at the optimal solution, we have $\text{Sign}(h_i) = \text{Sign}(f_i), \forall i$ or $\text{Sign}(h_i) = -\text{Sign}(f_i), \forall i$. Otherwise, we can also change the signs of corresponding f_i to satisfy this condition and improve the value of SNR. Also, we have $b_i = \text{abs}(f_i)\Delta$, for $\forall i$, at the optimal solution, otherwise we can increase $\text{abs}(f_i)$ to increase the value of the objective function in (41). Without loss of generality, we assume that $\text{Sign}(h_i) = \text{Sign}(f_i), \forall i$. The optimization problem in (41) reduces to

$$\begin{aligned} \max_{\mathbf{f},\mathbf{b}} \ & |\mathbf{f}^T\mathbf{h}|^2 \\ \text{s.t. } & \mathbf{1}^T\text{abs}(\mathbf{f}) \le \frac{P}{\Delta}. \end{aligned} \tag{42}$$

Let $\bar{f}_i = |f_i|$ and $\bar{h}_i = |h_i|$, the optimization problem in (42) is equivalent to

$$\begin{aligned} \max_{\bar{f}_i} \ & \sum_{i=1}^{N_t} \bar{f}_i\bar{h}_i \\ \text{s.t. } & \sum_{i=1}^{N_t} \bar{f}_i \le \frac{P}{\Delta}. \end{aligned} \tag{43}$$

Problem (43) is a linear programming problem, and its optimal solution is given by

$$\bar{f}_i^* = \begin{cases} \frac{P}{\Delta}, & i = \arg\max_k |h_k| \\ 0, & \text{other } i, \end{cases} \tag{44}$$

which further implies that the optimal solution of (41) has a form of

$$f_i^* = \begin{cases} \text{Sign}(h_i)\frac{P}{\Delta}, & i = \arg\max_k |h_k| \\ 0, & \text{other } i \end{cases} \tag{45}$$

and

$$b_i^* = \begin{cases} P, & i = \arg\max_k |h_k| \\ 0, & \text{other } i. \end{cases} \tag{46}$$

Unlike the RF case where the matched filter is the optimal beamformer for the MISO channel, here the optimal beamformer reduces to an LED selection scheme.

C. Complexity Analysis

In this section, we provide the complexity analysis of the proposed designs and compare with the zero-forcing (ZF) design [19]–[21]. In ZF precoding design, the computational complexity lies in computing the matrix multiplication and matrix inverse. According to the size of channel $\mathbf{H}$, the computational complexity can be denoted by $O(2N_r^2N_t + N_r^3)$. The main computational complexity of proposed SVD based design consists of computing the SVD decomposition and the monotonic optimization. The computational complexity of the former is $O(N_rN_t^2)$ [30]. As monotonic optimization is actually a polyblock approximation algorithm, the computational complexity can be expressed as $O(B(\frac{P}{\epsilon})^{N/c})$ where ϵ is the accuracy, B, P, and C are constants related to the class of objective in (21) [31]. Hence, the total computational complexity of the SVD based design can be approximated as $O\left(N_rN_t^2 + B(\frac{P}{\epsilon})^{N/c}\right)$. The computational complexity of the subgradient based design mainly includes computing $\nabla f(\mathbf{F})$ in (28) and m_k in (29), which implies that the total computational complexity can be approximated as $O\left(n_{ite}(N_r^2N_t + 3d^3 + N_r^2d)\right)$ where n_{ite} denotes the required number of iterations for the convergence. As for the MISO channel, the main computational complexity lies in finding the index i in (45), which has a complexity of $O(N_t)$. The above analysis reals that the proposed SVD based design and the subgradient based design generally have higher complexity than the ZF design, although they can bring certain performance improvement as shown in Section V.

IV. Joint Precoding and Offset Design for MIMO RGB VLC Systems

Recall that the information stream $\mathbf{d}$ is involved in the non-negative constraint $\mathbf{Fd} + \mathbf{b} \ge 0$ in (14). To get rid of the dependence on specific transmit symbols in $\mathbf{d}$, as in the white color case, we consider the worst case and replace it by $\mathbf{b} - \text{abs}(\mathbf{F})\mathbf{\Delta} \ge 0$, which is equivalent to

$$\triangle||\mathbf{e}_i^T\mathbf{F}||_1 - \mathbf{e}_i^T\mathbf{b} \le 0 \qquad \forall i, \tag{47}$$

where $\mathbf{e}_i$ is the i-th column of identity matrix $\mathbf{I}_{3N}$. Then optimization problem in (14) can be rewritten as

$$\min_{\mathbf{F},\mathbf{b}} \ \text{Tr}\left[\left(\mathbf{D}^{-1} + \frac{1}{\sigma^2}\mathbf{F}^T\mathbf{H}^T\mathbf{H}\mathbf{F}\right)^{-1}\right] \tag{48a}$$

$$\text{s.t. } \mathbf{b} \ge \mathbf{0} \tag{48b}$$

$$\triangle||\mathbf{e}_i^T\mathbf{F}||_1 - \mathbf{e}_i^T\mathbf{b} \le 0 \quad \forall i \tag{48c}$$

$$\mathbf{Jb} = P\bar{\mathbf{x}}. \tag{48d}$$

According to Lemma 1, optimization problem (48) is non-convex. It worth noting that as the results derived in Lemma 2 and Lemma 3 are not applicable in problem (48), we cannot reduce the number of the constraints in (48) as in (17). The subgradient based algorithm proposed for the white color case cannot be directly extended to the multiple color case due to the multiple constraints in (48). In what follows, we try to solve (48) by using some new transformations. That is, we optimize a new variable $\mathbf{Q} = \mathbf{FF}^T$ instead of $\mathbf{F}$. We first consider the case with $N = 3N_t$. The extension to a case with arbitrary N will be given at the end of this section. In order to solve $\mathbf{Q}$ instead of $\mathbf{F}$, we use the rule $\text{Tr}\left([\mathbf{I}_n + \mathbf{C}_{n\times m}\mathbf{D}_{m\times n}]^{-1}\right) = \text{Tr}\left([\mathbf{I}_m + \mathbf{D}_{m\times n}\mathbf{C}_{n\times m}]^{-1}\right) + n - m$ to transform the objective function to the

following form[2]

$$\begin{aligned}&\mathrm{Tr}\left[\left(\mathbf{D}^{-1}+\frac{1}{\sigma^2}\mathbf{F}^T\mathbf{H}^T\mathbf{H}\mathbf{F}\right)^{-1}\right]\\&=D\left\{\mathrm{Tr}\left[\left(\mathbf{I}+\frac{D}{\sigma^2}\mathbf{H}\mathbf{F}\mathbf{F}^T\mathbf{H}^T\right)^{-1}\right]+3N_t-3N_r\right\}\\&=D\left\{\mathrm{Tr}\left[\left(\mathbf{I}+\frac{D}{\sigma^2}\mathbf{H}\mathbf{Q}\mathbf{H}^T\right)^{-1}\right]+3N_t-3N_r\right\}.\end{aligned}\quad(49)$$

Further, using the relation $||\mathbf{e}_i^T\mathbf{F}||_1 \le \sqrt{3N_t}||\mathbf{e}_i^T\mathbf{F}||_2$, the constraint (48c) must be satisfied if the constraint

$$\triangle\sqrt{3N_t}||\mathbf{e}_i^T\mathbf{F}||_2-\mathbf{e}_i^T\mathbf{b}\le 0\quad(50)$$

is satisfied. As $b_i=\mathbf{e}_i^T\mathbf{b}\ge 0$, (50) is equivalent to

$$\triangle^2 3N_t\mathrm{diag}\{\mathbf{Q}\}_i-b_i^2\le 0.\quad(51)$$

Using (49) and (51), we modify the problem (50) into:

$$\min_{\mathbf{b},\mathbf{Q}\succeq\mathbf{0}}\ \mathrm{Tr}\left[\left(\mathbf{I}+\frac{D}{\sigma^2}\mathbf{H}\mathbf{Q}\mathbf{H}^T\right)^{-1}\right]\quad(52a)$$

$$\text{s.t. } b_i\ge 0\quad\forall i\quad(52b)$$

$$3N_t\triangle^2\mathrm{diag}(\mathbf{Q})_i\le b_i^2\quad\forall i\quad(52c)$$

$$\mathbf{1}^T\mathbf{b}_r=P\bar{x}_r,\ \mathbf{1}^T\mathbf{b}_g=P\bar{x}_g,\ \mathbf{1}^T\mathbf{b}_b=P\bar{x}_b\quad(52d)$$

where constraint (52d) is new expression of the constraint (48d). It is noted that optimization problem (52) is non-convex due to constraint (52c). To make (52) tractable, using the Taylor expansion, we approximate $f(b_i)=b_i^2$ as $f(b_i)=f(b_i^{(0)})+f'(b_i^{(0)})(b_i-b_i^{(0)})=2b_i^{(0)}b_i-b_i^{(0)2}$.[3] Using this approximation, the optimization problem (52c) changes into

$$\min_{\mathbf{b},\mathbf{Q}\succeq\mathbf{0}}\ \mathrm{Tr}\left[\left(\mathbf{I}+\frac{D}{\sigma^2}\mathbf{H}\mathbf{Q}\mathbf{H}^T\right)^{-1}\right]\quad(53a)$$

$$\text{s.t. } b_i\ge 0\quad\forall i\quad(53b)$$

$$\frac{3N_t\triangle^2}{2b_i^{(0)}}\mathrm{diag}(\mathbf{Q})_i+b_i^{(0)}/2\le b_i\quad\forall i\quad(53c)$$

$$\mathbf{1}^T\mathbf{b}_r=P\bar{x}_r,\ \mathbf{1}^T\mathbf{b}_g=P\bar{x}_g,\ \mathbf{1}^T\mathbf{b}_b=P\bar{x}_b.\quad(53d)$$

Optimization problem (53) is convex. Furthermore, we have the following observation.

Lemma 4: At the optimal solution of (53)*, constraint* (53c) *must be active, i.e.,* $\frac{3N_t\triangle^2}{2b_i^{(0)}}\mathrm{diag}(\mathbf{Q})_i+b_i^{(0)}/2=b_i$.

Proof: Please refer to Appendix B. □

Based on Lemma 4, we have the following problem

$$\begin{aligned}&\min_{\mathbf{b},\mathbf{Q}\succeq\mathbf{0}}\ \mathrm{Tr}\left[\left(\mathbf{I}+\frac{D}{\sigma^2}\mathbf{H}\mathbf{Q}\mathbf{H}^T\right)^{-1}\right]\\&\text{s.t. }\frac{3N_t\triangle^2}{2b_i^{(0)}}\mathrm{diag}(\mathbf{Q})_i+b_i^{(0)}/2=b_i,\quad\forall i\\&\qquad\mathbf{1}^T\mathbf{b}_r=P\bar{x}_r,\quad\mathbf{1}^T\mathbf{b}_g=P\bar{x}_g,\ \mathbf{1}^T\mathbf{b}_b=P\bar{x}_b.\end{aligned}\quad(54)$$

[2]It is noted that the transformation given in (49) requires that the range parameters D of different data streams are the same.

[3]This approximation is similar to one used in the difference of convex (DC) programming [24].

Let $\tilde{\mathbf{\Lambda}}_n$ be a diagonal matrix and $\tilde{\mathbf{\Lambda}}_n[i,i]=\frac{3N_t\triangle^2}{2b_{n,i}^{(0)}}$, $\mathbf{b}_n^{(0)}=[b_{n,1}^{(0)},b_{n,2}^{(0)},\cdots,b_{n,N}^{(0)}]$ with $n\in\{r,g,b\}$, optimization problem (54) is equivalent to

$$\begin{aligned}&\min_{\mathbf{Q}\succeq\mathbf{0}}\ \mathrm{Tr}\left[\left(\mathbf{I}+\frac{D}{\sigma^2}\mathbf{H}\mathbf{Q}\mathbf{H}^T\right)^{-1}\right]\\&\text{s.t. }\mathrm{Tr}(\mathbf{\Lambda}_r\mathbf{Q})\le\alpha_r\\&\qquad\mathrm{Tr}(\mathbf{\Lambda}_g\mathbf{Q})\le\alpha_g\\&\qquad\mathrm{Tr}(\mathbf{\Lambda}_g\mathbf{Q})\le\alpha_b\end{aligned}\quad(55)$$

where $\mathbf{\Lambda}_r=\mathrm{Blkdiag}(\tilde{\mathbf{\Lambda}}_r,\mathbf{0},\mathbf{0})$, $\mathbf{\Lambda}_g=\mathrm{Blkdiag}(\mathbf{0},\tilde{\mathbf{\Lambda}}_g,\mathbf{0})$, and $\mathbf{\Lambda}_b=\mathrm{Blkdiag}(\mathbf{0},\mathbf{0},\tilde{\mathbf{\Lambda}}_b)$; $\alpha_r=P\bar{x}_r-\frac{1}{2}\mathbf{1}^T\mathbf{b}_r^{(0)}$, $\alpha_g=P\bar{x}_g-\frac{1}{2}\mathbf{1}^T\mathbf{b}_g^{(0)}$, $\alpha_b=P\bar{x}_b-\frac{1}{2}\mathbf{1}^T\mathbf{b}_b^{(0)}$. The equivalence between (54) and (55) is due to the fact that the variables b_i can be discarded by combining the constraints in (54) and the fact that the optimal solution of (55) must activate all the constraints.

We now derive the optimal structure of $\mathbf{Q}$. Before that, we first give the following lemma.

Lemma 5: The optimal objective value of (55) *is lower-bounded by*

$$\begin{aligned}&q(\lambda_1,\lambda_2,\lambda_3)=\min_{\mathbf{Q}\succeq 0}\mathrm{Tr}\left[\left(\mathbf{I}+\frac{D}{\sigma^2}\mathbf{H}\mathbf{Q}\mathbf{H}^T\right)^{-1}\right]\\&s.t.\ \mathrm{Tr}\left\{(\lambda_1\mathbf{\Lambda}_r+\lambda_2\mathbf{\Lambda}_g+\lambda_3\mathbf{\Lambda}_b)\mathbf{Q}\right\}\\&\qquad\le\lambda_1\alpha_r+\lambda_2\alpha_g+\lambda_3\alpha_b\end{aligned}\quad(56)$$

where λ_1, λ_2 *and* λ_3 *are three non-negative scalars. Moveover, this lower bound is tight and can be achieved by* $\max_{\lambda_1,\lambda_2,\lambda_3}q(\lambda_1,\lambda_2,\lambda_3)$.

Proof: Since in Appendix B, we have proven that the objective function of (55) is convex. Thus, problem (55) is convex, which indicates that the Karush-Kuhn-Tucker (KKT) conditions are sufficient and necessary for deriving the optimal solution. Then, the proof of Lemma 5 is similar to the proof provided in [25, *Propositions 4 and 5*, which we omit for brevity. □

Denote $\mathbf{\Lambda}=\lambda_1\mathbf{\Lambda}_r+\lambda_2\mathbf{\Lambda}_g+\lambda_3\mathbf{\Lambda}_b$ and $\alpha=\lambda_1\alpha_r+\lambda_2\alpha_b+\lambda_3\alpha_b$. We reexpress (55) as

$$\begin{aligned}&\min_{\mathbf{Q}\succeq 0}\mathrm{Tr}\left[\left(\mathbf{I}+\frac{D}{\sigma^2}\mathbf{H}\mathbf{Q}\mathbf{H}^T\right)^{-1}\right]\\&s.t.\ \mathrm{Tr}\left\{\mathbf{\Lambda}\mathbf{Q}\right\}\le\alpha.\end{aligned}\quad(57)$$

For optimization problem (57), we have the following lemma.

Lemma 6: Let the SVD decomposition of $\mathbf{H}\mathbf{\Lambda}^{-1/2}$ *be* $\mathbf{H}\mathbf{\Lambda}^{-1/2}=\mathbf{U}\mathbf{D}\mathbf{V}^T$ *with* $\mathbf{D}=\mathrm{Diag}([d_1,d_2,\cdots,d_{3N_t}])$. *The optimal* $\mathbf{Q}$ *(denoted as* $\mathbf{Q}^*$*) has a structure of* $\mathbf{Q}^*=\mathbf{\Lambda}^{-1/2}\mathbf{V}\mathbf{\Lambda}_Q\mathbf{V}^T\mathbf{\Lambda}^{-1/2}$*, where* $\mathbf{\Lambda}_Q=\mathrm{Diag}\left([q_1,q_2,\cdots,q_{3N_t}]\right)$ *with* q_i *being given by*

$$q_i=\max\left(0,\frac{\sqrt{D\sigma^2d_i^2/\beta}-\sigma^2}{Dd_i^2}\right),\quad(58)$$

where $\beta\ge 0$ *is the Lagrange variable chosen to meet* $\sum_{i=1}^{3N_t}q_i=\alpha$.

Proof: Let $\bar{\mathbf{Q}} = \mathbf{\Lambda}^{1/2}\mathbf{Q}\mathbf{\Lambda}^{1/2}$, the optimization problem (57) becomes

$$\min_{\bar{\mathbf{Q}}\succeq 0} \mathrm{Tr}\left[\left(\mathbf{I}+\frac{D}{\sigma^2}\mathbf{H}\mathbf{\Lambda}^{-1/2}\bar{\mathbf{Q}}\mathbf{\Lambda}^{-1/2}\mathbf{H}^T\right)^{-1}\right] \quad (59)$$
$$s.t.\ \mathrm{Tr}\left\{\bar{\mathbf{Q}}\right\} \le \alpha.$$

Based on [23], the optimal structure of $\bar{\mathbf{Q}}$ has a form of $\bar{\mathbf{Q}}^* = \mathbf{V}\mathbf{\Lambda}_Q\mathbf{V}^T$ with $\mathbf{\Lambda}_Q = \mathrm{Diag}([q_1, q_2, \cdots, q_{3N_t}])$, which reduces (59) to the following power allocation problem

$$\min_{q_i\ge 0} \sum_{i=1}^{3N_t} \frac{\sigma^2}{\sigma^2 + Dd_i^2 q_i} \quad (60)$$
$$s.t.\ \sum_{i=1}^{3N_t} q_i \le \alpha.$$

By using the KKT conditions, the optimal solution of (60) can be proven to have a water-filling form given in (58), which completes the proof of Lemma 6. □

Similar to [25], Lemma 6 also implies that the optimal solution of (55) can be solved in an alternating manner, i.e., we can first solve problem (57) based on Lemma 6, and then update the variables λ_i, for $i = 1, 2, 3$, by using the subgradient based method. The optimal solution of (55) can be obtained upon convergence of the iteration.

With the obtained optimal solution of $\mathbf{Q}$ given in Lemma 5, we readily obtain the solution of $\mathbf{F}$ given as

$$\mathbf{F} = \mathbf{\Lambda}^{-1/2}\mathbf{V}\mathbf{\Lambda}_Q^{1/2}\mathbf{U}, \quad (61)$$

where $\mathbf{U}$ is an arbitrary $3N_t \times 3N_t$ unitary matrix. Note that in obtaining (61), we use certain approximations, which may not activate the power constraint (48c). We now scale $\mathbf{F}$ as follows to obtain the final solution

$$\mathbf{F}^* = \mathbf{\Xi}\mathbf{F}, \quad (62)$$

where $\mathbf{\Xi} = \begin{pmatrix} \tau_r\mathbf{I} & \mathbf{0} & \mathbf{0} \\ \mathbf{0} & \tau_g\mathbf{I} & \mathbf{0} \\ \mathbf{0} & \mathbf{0} & \tau_b\mathbf{I} \end{pmatrix}$ with scalars τ_r, τ_b, and τ_b being selected to activate the constraints in (48c). With $\mathbf{F}^*$, we update $\mathbf{b}$ using

$$\mathbf{b}^* = \mathrm{abs}(\mathbf{F}^*)\mathbf{\Delta}. \quad (63)$$

Based on the above analysis, the overall design algorithm is given in top of the left column of this page.

Now we discuss the case where the number of transmitted signal streams N is less than $3N_t$. In this case, matrix $\mathbf{F} \in \mathbb{R}^{3N_t\times N}$ is a tall matrix, which indicates that matrix $\mathbf{Q} = \mathbf{F}\mathbf{F}^T$ introduced in (52) is not full-rank. If the number of data streams sent from the transmitter is d, the rank of $\mathbf{Q}$ is d. Problem (52) becomes

$$\min_{\mathbf{b},\mathbf{Q}\succeq\mathbf{0}} \mathrm{Tr}\left[\left(\mathbf{I}+\frac{D}{\sigma^2}\mathbf{H}\mathbf{Q}\mathbf{H}^T\right)^{-1}\right] \quad (64a)$$
$$\text{s.t. } b_i \ge 0 \quad \forall i \quad (64b)$$
$$3N_t\triangle^2\mathrm{diag}(\mathbf{Q})_i \le b_i^2 \quad \forall i \quad (64c)$$
$$\mathbf{1}^T\mathbf{b}_r = P\bar{x}_r,\ \mathbf{1}^T\mathbf{b}_g = P\bar{x}_g,\ \mathbf{1}^T\mathbf{b}_b = P\bar{x}_b \quad (64d)$$
$$\mathrm{rank}(\mathbf{Q}) = d. \quad (64e)$$

Algorithm 2

- **Repeat**
  - **Solve** the problem (57) for fixed $\lambda_i(n), i = 1, 2, 3$ using Lemma 6.
  - **Update** the variables $\lambda_1(n), \lambda_2(n), \lambda_3(n)$ using the subgradient-based method[4]

$$\lambda_1(n+1) = \lambda_1(n) - \Delta_n(\alpha_r - \mathrm{Tr}(\mathbf{\Lambda}_r\mathbf{Q}^*(n)),$$
$$\lambda_2(n+1) = \lambda_2(n) - \Delta_n(\alpha_g - \mathrm{Tr}(\mathbf{\Lambda}_g\mathbf{Q}^*(n)),$$
$$\lambda_3(n+1) = \lambda_3(n) - \Delta_n(\alpha_b - \mathrm{Tr}(\mathbf{\Lambda}_b\mathbf{Q}^*(n)).$$

- **Update** b_i based on Lemma 4.
- **Update** $b_i^{(0)}$ in (53) by setting $b_i^{(0)} = b_i$.
- **Until** termination criterion is satisfied, obtain $\mathbf{F}$ and $\mathbf{b}$ using (62) and (63).

Note that since the rank constraint (64e) is non-convex, the previously proposed algorithm is not applicable. To obtain a solution of (64), we may relax it by ignoring the rank constraint (64e) by directly solving problem (52). After getting a solution $\mathbf{Q}$, denoted as $\mathbf{Q}^*$ and assuming the SVD decomposition of $\mathbf{Q}^*$ as $\mathbf{U}_Q\mathbf{\lambda}_Q\mathbf{U}_Q^T$ where $\mathbf{U}_Q$ is $3N_t \times 3N_t$ unitary matrix and $\mathbf{\lambda}_Q$ is $3N_t \times 3\tilde{N}_t$ diagonal singular value matrix, the solution $\mathbf{F}$ can be obtained as

$$\mathbf{F}_d^* = \mathbf{U}_Q\mathbf{\lambda}_Q^d\mathbf{V}_Q, \quad (65)$$

where $\mathbf{\lambda}_Q^d = \mathbf{\lambda}_Q(:, 1:d)$ and $\mathbf{V}_Q$ is an arbitrary $d \times d$ unitary matrix. It is worth noting that matrix $\mathbf{F}_d^*\mathbf{F}_d^{*T}$ satisfies constraint (64c).

The complexity of the joint design in the MIMO RGB VLC system mainly includes computing SVD and q_i in Lemma 6 during each iteration of Algorithm 2 and computing $\mathbf{F}$ in (61). The complexity of computing SVD is $O(9N_t^2)$. To compute q_i in (58), we use bisection search to determine parameter β with a complexity of $O(\log_2(\frac{\alpha}{\varepsilon}))$ where ε denotes the accuracy. The complexity computing $\mathbf{F}$ in (61) can be denoted as $O(9N_t^2)$. The total complexity can be represented as $O\left(n_{ite}(9N_t^2 + \log_2(\frac{\alpha}{\varepsilon})) + 9N_t^2\right)$ where n_{ite} denotes the required iteration number for the convergence of Algorithm 2.

V. Simulation Results

In this section, we present some simulation results to evaluate the performance of the proposed designs. To this end, we first present how to generate practical VLC channels in our simulations.

A. Channel Model

In this subsection, we provide the details of system configuration and parameters in our simulations. We consider a typical medium-size cubic room with a size of 5m × 5m × 3m where 3m is the room height.

For the white VLC case, we assume that there are five transmit LEDs located on the ceiling and three PDs performing

[4]The subgradient can be found as in [25] and the step size can be chosen as in [26].

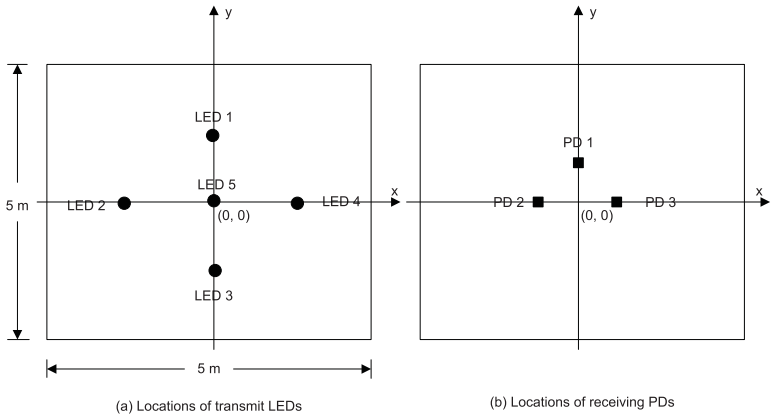

Fig. 1. The layout of transmit LEDs and receiving PDs.

as receiving photodetectors positioned at a height of 1m above the floor. The layout of transmit LEDs and receiving PDs is illustrated in Fig. 1, where the coordinates of five transmit LEDs are given as: LED 1 $\Rightarrow$ $(x, y) = (0, 1.5)$, LED 2 $\Rightarrow$ $(x, y) = (-1.5, 0)$, LED 3 $\Rightarrow$ $(x, y) = (0, -1.5)$, LED 4 $\Rightarrow$ $(x, y) = (1.5, 0)$, and LED 5 $\Rightarrow$ $(x, y) = (0, 0)$; the coordinates of three receiving PDs are given as: PD 1 $\Rightarrow$ $(x, y) = (0, 1)$, PD 2 $\Rightarrow$ $(x, y) = (-1, 0)$, and PD 3 $\Rightarrow$ $(x, y) = (1, 0)$. Following existing works in [33]–[36], we assume that the channel from a transmit LED to a receiving PD includes the line-of-sight (LOS) link and reflection links. In specific, the channel from LED i to PD j is denoted as

$$h_{ji}(t) = h^{ji}_{\text{LOS}}(t) + h^{ji}_{\text{ref}}(t), \tag{66}$$

where $h^{ji}_{\text{LOS}}(t)$ and $h^{ji}_{\text{ref}}(t)$ denote the channel gain of LOS link and reflection link, respectively. $h^{ji}_{\text{LOS}}(t)$ is determined by the LED radiation pattern, the effective area of the receiving PD, and its location to the LEDs. On the other hand, $h^{ji}_{\text{ref}}(t)$ is determined by the multiple reflections, which implies

$$h^{ji}_{\text{ref}}(t) = \sum_{k=1}^{K} h^{k}_{ji}(t), \tag{67}$$

where $h^{k}_{ji}(t)$ denotes the channel gain with k bounce reflection and K denotes the maximum number of bounces. In our scenario, we assume $K = 1$, implying that $h^{ji}_{\text{ref}}(t)$ consists of 1 bounce due to plaster wall reflection or the floor reflection. According to [33]–[36], $h^{ji}_{\text{LOS}}(t)$ and $h^{ji}_{\text{ref}}(t)$ can be expressed, respectively, by

$$\begin{aligned} h^{ji}_{\text{LOS}}(t) &= \frac{\mathcal{A}^{j}_{\text{PD}}(m+1)\cos^{m}\phi^{ji}_{0}\cos\theta^{ji}_{0}}{2\pi {d^{ji}_{0}}^{2}}\text{rect}\left(\frac{\theta^{ji}_{0}}{\text{FOV}}\right) \\ &\quad \times \delta(t - \frac{d^{ji}_{0}}{c}) \\ h^{ji}_{\text{ref}}(t) &= L^{ji}_{\text{wa},1}L^{ji}_{\text{wa},2}\Gamma_{\text{wa}}\text{rect}\left(\frac{\theta^{ji}_{\text{wa},2}}{\text{FOV}}\right)\delta(t - \frac{d^{ji}_{\text{wa},1} + d^{ji}_{\text{wa},2}}{c}) \\ &\quad + L^{ji}_{\text{fl},1}L^{ji}_{\text{fl},2}\Gamma_{\text{fl}}\text{rect}\left(\frac{\theta^{ji}_{\text{fl},2}}{\text{FOV}}\right)\delta(t - \frac{d^{ji}_{\text{fl},1} + d^{ji}_{\text{fl},2}}{c}), \end{aligned} \tag{68}$$

where $\mathcal{A}^{j}_{\text{PD}}$ is the active area of the PD j, $m = \frac{-1}{\log_2(\cos(\phi_{1/2}))}$ denotes the number of a radiation lobe used for measuring the directivity of the light beam relating to the semi-angle at half-power $\phi_{1/2}$; ϕ^{ji}_{0} and θ^{ji}_{0} are the angles of irradiance and incidence in LOS link, respectively; d^{ji}_{0} denotes the distance of LOS link; c denotes the speed of light; FOV is the filed of view; Γ_{wa} and Γ_{fl} denote the reflection parameters of the wall and the floor, respectively; $\theta^{ji}_{\text{wa},n}$ and $\theta^{ji}_{\text{fl},n}$ denote the incidence angles of the n-th hop in the wall reflection link and the floor reflection link, respectively; $d^{ji}_{\text{wa},n}$ and $d^{ji}_{\text{fl},n}$ denote the distances of the n-th hop in the wall reflection link and the floor reflection link, respectively; $L^{ji}_{\text{wa},n}$ and $L^{ji}_{\text{fl},n}$ are given by

$$\begin{aligned} L^{ji}_{\text{wa},1} &= \frac{\mathcal{A}^{ji}_{\text{wa,ref}}(m+1)\cos^{m}\phi^{ji}_{\text{wa},1}\cos\theta^{ji}_{\text{wa},1}}{2\pi {d^{ji}_{\text{wa},1}}^{2}} \\ L^{ji}_{\text{wa},2} &= \frac{\mathcal{A}^{j}_{\text{PD}}\cos\phi^{ji}_{\text{wa},2}\cos\theta^{ji}_{\text{wa},2}}{2\pi {d^{ji}_{\text{wa},2}}^{2}} \\ L^{ji}_{\text{fl},1} &= \frac{\mathcal{A}^{ji}_{\text{fl,ref}}(m+1)\cos^{m}\phi^{ji}_{\text{fl},1}\cos\theta^{ji}_{\text{fl},1}}{2\pi {d^{ji}_{\text{fl},1}}^{2}} \\ L^{ji}_{\text{fl},2} &= \frac{\mathcal{A}^{j}_{\text{PD}}\cos\phi^{ji}_{\text{fl},2}\cos\theta^{ji}_{\text{fl},2}}{2\pi {d^{ji}_{\text{fl},2}}^{2}} \end{aligned} \tag{69}$$

where $\mathcal{A}^{ji}_{\text{wa,ref}}$ and $\mathcal{A}^{ji}_{\text{fl,ref}}$ denote the activate area of the wall reflection and floor reflection, respectively; $\phi^{ji}_{\text{wa},n}$ and $\phi^{ji}_{\text{fl},n}$ denote the irradiance angles of the n-th hop in the wall reflection link and the floor reflection link, respectively. Other simulation parameters are list in Table I. With the above channel modeling, the delay spread of the channel can be denoted by

$$\tau = \max_{ji}\tau_{ji} = \max_{ji}\max\{\frac{d^{ji}_{0}}{c}, \frac{d^{ji}_{\text{wa},1} + d^{ji}_{\text{wa},2}}{c}, \frac{d^{ji}_{\text{fl},1} + d^{ji}_{\text{fl},2}}{c}\}. \tag{70}$$

In our considered case, it is not hard to obtain $\tau \leq 3.47$ns. We assume that the data rate of our considered system is not larger than 30Mb/s. In this case, the delay spread is less than $\frac{1}{10}$ of symbol duration. Therefore, the impact of delay spread can be ignored and the equalization technique is not required in our considered system.

TABLE I
SIMULATION PARAMETERS

Parameter	Value
Semi-angle at half-power $\phi_{1/2}$	80^o
PD active area $\mathcal{A}_{\rm PD}^{j}$	$1\ {\rm cm}^2$
Receiving FOV	80^o
Wall reflectivity(plaster) $\Gamma_{\rm wa}$	0.82
Floor reflectivity $\Gamma_{\rm fl}$	0.61
Wall reflection area $\mathcal{A}_{\rm wa,ref}^{ji}$	$1\ {\rm cm}^2$
Floor reflection area $\mathcal{A}_{\rm fl,ref}^{ji}$	$1\ {\rm cm}^2$

For the MIMO RGB VLC case, we assume that the layout of the transmit LEDs and receiving PDs is the same with one shown in Fig. 1. In specific, each LED (or each PD) in Fig. 1 consists of multi-color chips, i.e., red, green, and blue chips, (or multi-color detection chips). For each individual color band, the channel model is similar to (66). The only difference is the reflectivity parameters which are different for different color bands. Denote by $\Gamma_{{\rm wa},c}$ the wall reflectivity parameter in color band c and by $\Gamma_{{\rm fl},c}$ the floor reflectivity parameter in color band c. We set $\Gamma_{{\rm wa},r}=0.9$, $\Gamma_{{\rm wa},g}=0.85$, $\Gamma_{{\rm wa},b}=0.82$, $\Gamma_{{\rm fl},r}=0.8$, $\Gamma_{{\rm fl},r}=0.7$, $\Gamma_{{\rm fl},b}=0.61$. Furthermore, we consider multi-color interaction (also known as cross-talk) due to imperfect optical filter in PDs. The overall channel matrix in MIMO RGB VLC is given by

$$\mathbf{H}_{rgb}=\begin{pmatrix}(1-\xi)\mathbf{H}_r & \xi\mathbf{H}_g & \mathbf{0}\\ \xi\mathbf{H}_r & (1-2\xi)\mathbf{H}_g & \xi\mathbf{H}_b\\ \mathbf{0} & \xi\mathbf{H}_g & (1-\xi)\mathbf{H}_b\end{pmatrix} \quad (71)$$

where $\mathbf{H}_c\in\mathbb{R}^{N_r\times N_t}$, $c\in\{R,G,B\}$, denote the channel matrix in color band c with perfect perfect optical filter, and $\xi\in(0,0.5]$ characterizes the interference ratio. To obtain channel matrix (71), we assume that the signal leakage only occurs between two neighboring color bands due to their close frequencies.

B. Performance Evaluations

In Figs. 2 (a) and (b), we show the normalized MSE and uncoded bit-error-rate (BER) comparison between the proposed two designs and the ZF precoding design with the change of power at $N_t=N_r=3$. In specific, the first three LEDs (i.e., LED 1, 2, and 3) in Fig. 1 (a) are chosen as transmit LEDs. When simulating the BER performance, we assume that 4-PAM modulated symbols are used and the constellation of 4-PAM is formed in the range of $[-3,3]$, i.e., $\triangle=3$. It is observed that both the proposed SVD based precoding design and gradient based design significantly outperform the ZF precoding design. Furthermore, the proposed gradient based design outperforms the SVD based design since no suboptimal structure is imposed on the precoding matrix in the gradient based design.

Figure 3 (a) and (b) illustrates the normalized MSE and uncoded BER comparison between the proposed design and the uniform design for MISO white VLC systems, where 'Uniform beamforming' means that identical powers are distributed among all transmit LEDs to transmit single symbol. Here we assume that the first PD (i.e., PD 1) in Fig. 1 (b) is chosen as the single receiving PD, and for the simulation with $N_t=2$, the last three LEDs (i.e., LED 4, and 5) in Fig. 1 (a) are chosen as transmit LEDs. We observe that the proposed optimal design largely outperforms the 'Uniform beamforming', and this performance enhancement is increased as the increase of the number of transmit LEDs. This is because increased number of transmit LEDs offers us more selection diversity. Furthermore, by comparing with the multiple-data-stream transmission in Figs. 2 (a) and (b), we observe that higher diversity orders can be obtained in Figs. 3 (a) and (b) when transmitting single data stream due to diversity-multiplexing tradeoff.

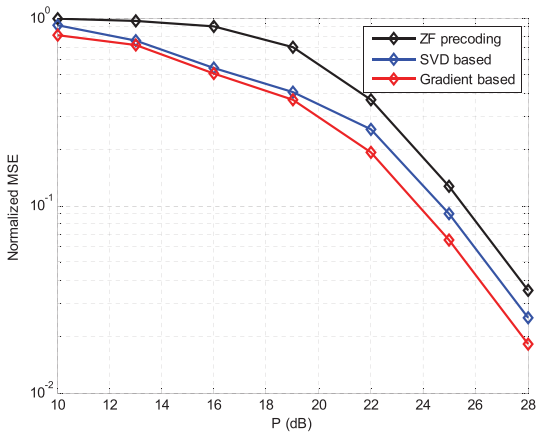

(a) MSE

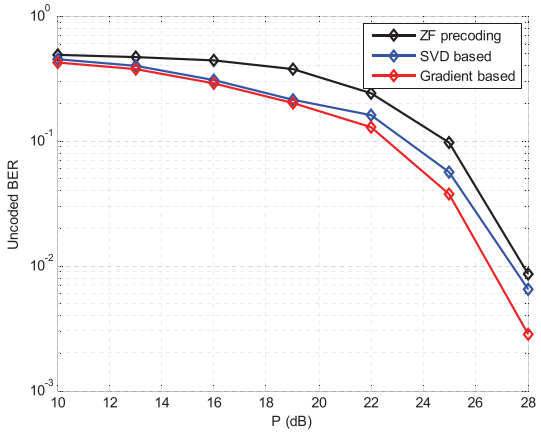

(b) Uncoded BER

Fig. 2. Performance comparison between the proposed designs and ZF bemaforming design for the MIMO white VLC system.

Figure 4 illustrates the convergence behavior of updating $\{\lambda_1,\lambda_2,\lambda_3\}$, i.e., the convergence of Algorithm 2, for one random channel realization at $N_t=2$ and $P=10$ dB. We find that in general, the update of $\{\lambda_1,\lambda_2,\lambda_3\}$ converges fast, and almost 10 iterations are enough for the convergence.

For the MIMO RGB VLC systems, we illustrate the performance of the normalized MSE and uncoded BER in Figs. 5 (a) and (b), respectively, with $N_t=N_r=3$. Also, here we choose the first three LEDs (i.e., LED 1, 2, and 3) in Fig. 1 (a) as transmit LEDs. Specifically, the value of $\bar{\mathbf{x}}=[\bar{x}_r,\bar{x}_g,\bar{x}_b]$ in the left subfigure and the right subfigure of Figs. 5 (a) and (b) are chosen as $[0.7,0.15,0.15]$

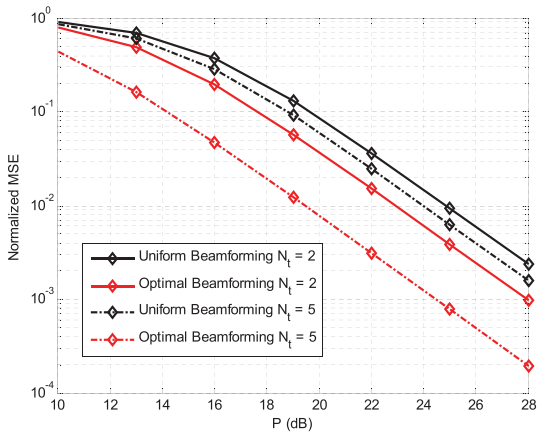

(a) MSE

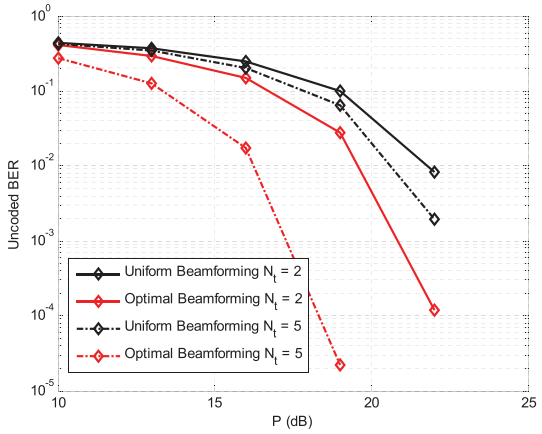

(b) Uncoded BER

Fig. 3. Performance comparison between the proposed optimal design and uniform bemaforming design for the MISO white VLC system.

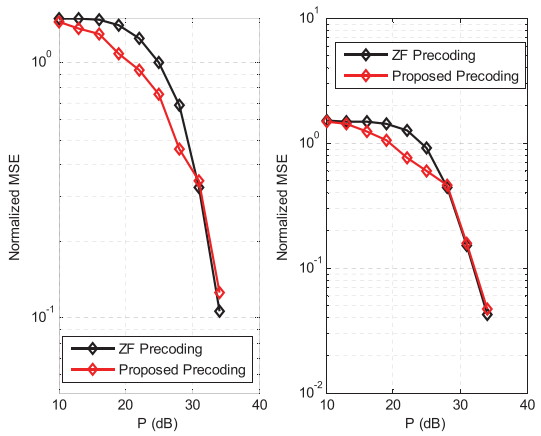

(a) MSE

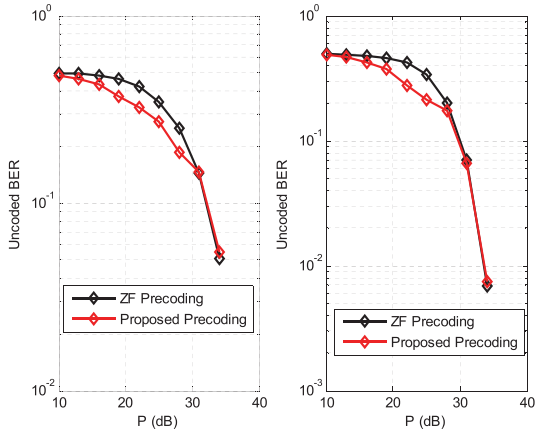

(b) Uncoded BER

Fig. 5. Performance comparison between the proposed designs and ZF bemaforming design for the MIMO RGB VLC system.

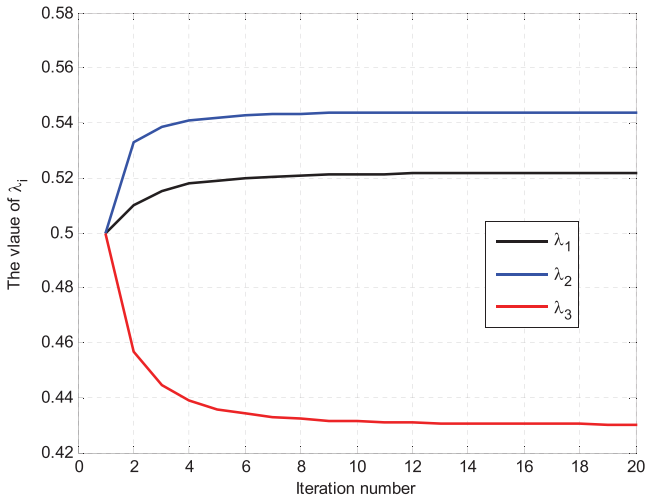

Fig. 4. Illustration of the convergence behavior of $\{\lambda_1, \lambda_2, \lambda_3\}$.

and $[\frac{4}{9}, \frac{3}{9}, \frac{2}{9}]$, respectively. We find that the later has a more balanced color illumination setting than the former one. The curves in Figs. 5 (a) and (b) verify the superiority of the proposed design over the ZF precoding in low to medium SNR regimes, but they get a close performance in high SNR regime. The reason is that when SNR is high, the power of the noise is less compared to the high transmit power. In this case, the noise amplification due to the nature of ZF precoding can be ignored, which makes the ZF precoding a good design in VLC systems. Also, the approximation used in our design may incur performance loss in high SNR regime. The curves in Figs. 5 (a) and (b) further indicate that a system with balanced color illumination setting performs better than a system with unbalanced color illumination setting. This result is expected since compared to the balanced color illustration system, the unbalanced one allocates less power to green and blue color branches, the insufficient power allocation (e.g. to G color and B color) could result in performance degradations if the channel gains among three color branches are not different too much.

VI. Conclusion

In this paper, we studied the joint precoding and offset optimization for the VLC systems with multiple transmit LEDs. Some important properties were first proven to simplify the design problems. Based on these properties, we developed two design algorithms for the MIMO white VLC systems. For the MISO white VLC systems, we proved that the optimal precoding reduces to a simple LED selection scheme, which is very different from the traditional MISO RF communications.

By performing certain approximations on the original design problem, the optimal beamforming structure was derived for the MIMO RGB VLC systems. Various simulation results were presented to verify the effectiveness of the proposed designs.

APPENDIX A
PROOF OF LEMMA 1

The nonconvexity of (15) can be proven by showing that the objective function is nonconvex or the feasible region formed by the constraints is nonconvex. It is easy to verify that the feasible region in (15) is convex. Next we show that the objective function of (15) is nonconvex, which results in the nonconvexity of (15). As $\mathrm{Tr}\left[\left(\mathbf{D}^{-1}+\frac{1}{\sigma^2}\mathbf{F}^T\mathbf{H}^T\mathbf{H}\mathbf{F}\right)^{-1}\right]=D\mathrm{Tr}\left[\left(\mathbf{I}+\frac{D}{\sigma^2}\mathbf{F}^T\mathbf{H}^T\mathbf{H}\mathbf{F}\right)^{-1}\right]$, proving the nonconvexity of the objective function of (15) is equivalent to proving the nonconvexity of $g(\mathbf{F})=\mathrm{Tr}\left[\left(\mathbf{I}+\frac{D}{\sigma^2}\mathbf{F}^T\mathbf{H}^T\mathbf{H}\mathbf{F}\right)^{-1}\right]$. To this end, we define $f(\alpha)=g\left(\alpha\mathbf{F}_1+(1-\alpha)\mathbf{F}_2\right)$. According to [27], the convexity of $g(\mathbf{F})$ implies that $\frac{\partial^2 f(\alpha)}{\partial^2\alpha}\geq 0$.

The second order derivative of $f(\alpha)$ with respect to α is given by

$$\frac{\partial^2 f(\alpha)}{\partial^2\alpha}=2\mathrm{Tr}(\mathbf{A}^{-1}\frac{\partial\mathbf{A}}{\partial\alpha}\mathbf{A}^{-1}\frac{\partial\mathbf{A}}{\partial\alpha}\mathbf{A}^{-1})-\mathrm{Tr}(\mathbf{A}^{-1}\frac{\partial^2\mathbf{A}}{\partial^2\alpha}\mathbf{A}^{-1}), \tag{72}$$

where we define

$$\begin{aligned}\mathbf{A}&=\mathbf{I}+\frac{D}{\sigma^2}[\alpha\mathbf{F}_1+(1-\alpha)\mathbf{F}_2]^T\mathbf{H}^T\mathbf{H}[\alpha\mathbf{F}_1+(1-\alpha)\mathbf{F}_2],\\ \frac{\partial\mathbf{A}}{\partial\alpha}&=2\frac{D}{\sigma^2}\alpha\mathbf{F}_3^T\mathbf{H}^T\mathbf{H}\mathbf{F}_3+\frac{D}{\sigma^2}\mathbf{F}_3^T\mathbf{H}^T\mathbf{H}\mathbf{F}_2+\frac{D}{\sigma^2}\mathbf{F}_2^T\mathbf{H}^T\mathbf{H}\mathbf{F}_3,\\ \frac{\partial^2\mathbf{A}}{\partial^2\alpha}&=2\frac{D}{\sigma^2}\mathbf{F}_3^T\mathbf{H}^T\mathbf{H}\mathbf{F}_3,\end{aligned} \tag{73}$$

with $\mathbf{F}_3=\mathbf{F}_1-\mathbf{F}_2$. Substituting (73) into (72), we see that $\frac{\partial^2 f(\alpha)}{\partial^2\alpha}$ cannot be always positive. The sign of $\frac{\partial^2 f(\alpha)}{\partial^2\alpha}$ actually depends on the value of α, $\mathbf{H}$, $\mathbf{F}_1$, and $\mathbf{F}_2$. We thus conclude that $f(\alpha)$ is not convex in $\mathbf{F}$, which further indicates the nonconvexity of (15).

APPENDIX B
PROOF OF LEMMA 4

To prove Lemma 4, we first prove that function $h(\mathbf{Q})=\mathrm{Tr}\left[\left(\mathbf{I}+\frac{D}{\sigma^2}\mathbf{H}\mathbf{Q}\mathbf{H}^T\right)^{-1}\right]$ is convex with respect to semidefinite positive matrix $\mathbf{Q}$. To this goal, we define $g(\alpha)=g(\alpha\mathbf{Q}_1+(1-\alpha)\mathbf{Q}_2)$ where $\mathbf{Q}_1$ and $\mathbf{Q}_2$ are $3N\times 3N$ real symmetric matrices. Its second order derivative with respect to α is denoted as

$$\frac{\partial^2 g(\alpha)}{\partial^2\alpha}=2\mathrm{Tr}(\mathbf{B}^{-1}\frac{\partial\mathbf{B}}{\partial\alpha}\mathbf{B}^{-1}\frac{\partial\mathbf{B}}{\partial\alpha}\mathbf{B}^{-1})-\mathrm{Tr}(\mathbf{B}^{-1}\frac{\partial^2\mathbf{B}}{\partial^2\alpha}\mathbf{B}^{-1})$$

where $\mathbf{B}=\mathbf{I}+\frac{D}{\sigma^2}\mathbf{H}(\alpha\mathbf{Q}_1+(1-\alpha)\mathbf{Q}_2)\mathbf{H}^T$. Since $\frac{\partial^2\mathbf{B}}{\partial^2\alpha}=0$ and $2\mathrm{Tr}(\mathbf{B}^{-1}\partial\mathbf{B}\mathbf{B}^{-1}\partial\mathbf{B}\mathbf{B}^{-1})\geq 0$, $\frac{\partial^2 g(\alpha)}{\partial^2\alpha}$ is positive. Therefore, $h(\mathbf{Q})$ is convex in $\mathbf{Q}$.

Now we prove Lemma 4 using contradiction. If the optimal solution of (53), $\mathbf{Q}_{opt}$, does not activate constraint (53c) for certain i. We can always generate a new $\mathbf{Q}'=\mathbf{Q}_{opt}+a\mathbf{e}_i\mathbf{e}_i^T$ where a is a nonnegative value satisfying $\frac{3N_t\triangle^2}{2b_i^{(0)}}[\mathrm{diag}(\mathbf{Q})_i+a]+b_i^{(0)}/2=b_i$. It is noted that as $\mathbf{Q}'\succeq\mathbf{Q}_{opt}$, we have $\mathbf{I}+\frac{D}{\sigma^2}\mathbf{H}\mathbf{Q}'\mathbf{H}^T\succeq\mathbf{I}+\frac{D}{\sigma^2}\mathbf{H}\mathbf{Q}_{opt}\mathbf{H}^T$, then $\left(\mathbf{I}+\frac{D}{\sigma^2}\mathbf{H}\mathbf{Q}_{opt}\mathbf{H}^T\right)^{-1}\succeq\left(\mathbf{I}+\frac{D}{\sigma^2}\mathbf{H}\mathbf{Q}'\mathbf{H}^T\right)^{-1}$, which implies $h(\mathbf{Q}')\leq h(\mathbf{Q}_{opt})$. This contradicts the optimality assumption of $\mathbf{Q}_{opt}$. We thus complete the proof of Lemma 4.

REFERENCES

[1] Q. Gao, R. Wang, Z. Xu, and Y. Hua, "Joint beamformer and offset design for multi-color visible light communications," *IEEE WCSP*, Hefei, China, Oct. 2014, pp. 1–6.

[2] T. Komine and M. Nakagawa, "Fundamental analysis for visible-light communication system using LED lights," *IEEE Trans. Consum. Electron.*, vol. 50, no. 1, pp. 100–107, Feb. 2004.

[3] S. Rajagopal, R. D. Roberts, and S.-K. Lim, "IEEE 802.15.7 visible light communication: Modulation schemes and dimming support," *IEEE Commun. Mag.*, vol. 50, no. 3, pp. 72–82, Mar. 2012.

[4] H. Elgala, R. Mesleh, and H. Haas, "Indoor optical wireless communication: Potential and state-of-the-art," *IEEE Commun. Mag.*, vol. 49, no. 9, pp. 56–63, Sep. 2011.

[5] *Colour Rendering, TC 1-33 Closing Remarks*, CIE Central Bureau, Vienna, Austria, 1999.

[6] *IEEE Standard for Local and Metropolitan Area Networks—Part 15.7: Short-Range Wireless Optical Communication Using Visible Light*, IEEE Standard 802.15.7, Sep. 2011.

[7] R. Mesleh, H. Elgala, and H. Haas, "Optical spatial modulation," *IEEE J. Opt. Commun. Netw.*, vol. 3, no. 3, pp. 234–244, Mar. 2011.

[8] S. Dimitrov, S. Sinanovic, and H. Haas, "Signal shaping and modulation for optical wireless communication," *J. Lightw. Technol.*, vol. 30, no. 9, pp. 1319–1328, May 1, 2012.

[9] A. Stimson, *Photometry Radiometry for Engineers*. New York, NY, USA: Wiley, 1974.

[10] J. Armstrong, "OFDM for optical communications," *J. Lightw. Technol.*, vol. 27, no. 3, pp. 189–204, Feb. 1, 2009.

[11] H. Elgala, R. Mesleh, and H. Haas, "Indoor broadcasting via white LEDs and OFDM," *IEEE Trans. Consum. Electron.*, vol. 55, no. 3, pp. 1127–1134, Aug. 2009.

[12] I. Stefan, H. Elgala, and H. Haas, "Study of dimming and LED nonlinearity for ACO-OFDM based VLC systems," in *Proc. IEEE WCNC*, Paris, France, Apr. 2012, pp. 990–994.

[13] Q. Gao, J. H. Manton, G. Chen, and Y. Hua, "Constellation design for a multicarrier optical wireless communication channel," *IEEE Trans. Commun.*, vol. 62, no. 1, pp. 214–225, Jan. 2014.

[14] M. Beko and R. Dinis, "Systematic method for designing constellations for intensity-modulated optical systems," *IEEE Opt. Communi. Netw.*, vol. 6, no. 5, pp. 449–458, May 2014.

[15] L. Zeng *et al.*, "High data rate multiple input multiple output (MIMO) optical wireless communications using white led lighting," *IEEE J. Sel. Areas Commun.*, vol. 27, no. 9, pp. 1654–1662, Dec. 2009.

[16] C. Gong, S. Li, Q. Gao, and Z. Xu, "Power and rate optimization for visible light communication system with lighting constraints," *IEEE Trans. Signal Process.*, vol. 63, no. 16, pp. 4245–4256, Aug. 2015.

[17] K.-H. Park, Y.-C. Ko, and M.-S. Alouini, "On the power and offset allocation for rate adaptation of spatial multiplexing in optical wireless MIMO channels," *IEEE Trans. Commun.*, vol. 61, no. 4, pp. 1535–1543, Apr. 2013.

[18] K. Ying, H. Qian, R. J. Baxley, and S. Yao, "Joint optimization of precoder and equalizer in MIMO VLC systems," *IEEE J. Sel. Areas Commun.*, vol. 33, no. 9, pp. 1949–1958, Sep. 2015.

[19] Z. Yu, R. J. Baxley, and G. T. Zhou, "Multi-user MISO broadcasting for indoor visible light communication," in *Proc. IEEE ICASSP*, Vancouver, BC, Canada, May 2013, pp. 4849–4853.

[20] H. Shen, Y. Deng, W. Xu, and C. Zhao, "Rate-maximized zero-forcing beamforming for VLC multiuser MISO downlinks," *IEEE Photon. J.*, vol. 8, no. 1, pp. 1–13, Feb. 2016.

[21] H. Ma, L. Lampe, and S. Hranilovic, "Robust MMSE linear precoding for visible light communication broadcasting systems," in *Proc. IEEE Globecom Workshop*, Atlanta, GA, USA, Dec. 2013, pp. 1081–1086.

[22] R. Feng, M. Dai, H. Wang, B. Chen, and X. Lin, "Linear precoding for multiuser visible-light communication with field-of-view diversity," *IEEE Photon. J.*, vol. 8, no. 2, Apr. 2016, Art. no. 7902708.

[23] D. P. Palomar, J. M. Cioffi, and M. A. Lagunas, "Joint Tx-Rx beamforming design for multicarrier MIMO channels: A unified framework for convex optimization," *IEEE Trans. Signal Process.*, vol. 51, no. 9, pp. 2381–2401, Sep. 2003.
[24] A. L. Yuille and A. Rangarajan, "The concave-convex procedure," *Neural Comput.*, vol. 15, no. 4, pp. 915–936, 2003.
[25] L. Zhang, R. Zhang, Y.-C. Liang, Y. Xin, and H. V. Poor, "On Gaussian MIMO BC-MAC duality with multiple transmit covariance constraints," *IEEE Trans. Inf. Theory*, vol. 58, no. 4, pp. 2064–2078, Apr. 2012.
[26] S. Boyd, L. Xiao, and A. Mutapcic, "Subgradient methods," Stanford Univ., Stanford, CA, USA, Tech. Rep. EE354b, 2008.
[27] S. Boyd and L. Vandenberghe, *Convex Optimization*. Cambridge, U.K.: Cambridge Univ. Press, 2004.
[28] D. P. Bertsekas, *Nonlinear Programming*, Belmont, MA, USA: Athena Scientific, 1995.
[29] Y. Zhang, L. Qian, and J. Huang, "Monotonic optimization in communication and networking systems," *Found. Trends Netw.*, vol. 7, no. 1, pp. 1–75, Oct. 2012.
[30] J. B. Fraleigh and R. A. Beauregard, *Linear Algebra*. Reading, MA, USA: Addison-Wesley, 1987.
[31] J. Brehmer, *Utility Maximization in Nonconvex Wireless Systems*. Berlin, Germany: Springer, 2012.
[32] M. Tao and R. Wang, "Robust relay beamforming for two-way relay networks," *IEEE Commun. Lett.*, vol. 16, no. 7, pp. 1052–1055, Jul. 2012.
[33] K. Lee, H. Park, and J. R. Barry, "Indoor channel characteristics for visible light communications," *IEEE Commun. Lett.*, vol. 15, no. 2, pp. 217–219, Feb. 2011.
[34] F. Miramirkhani and M. Uysal, "Channel modeling and characterization for visible light communications," *IEEE Photon. J.*, vol. 7, no. 6, Dec. 2015, Art. no. 7905616.
[35] S. Long, M.-A. Khalighi, M. Wolf, S. Bourennane, and Z. Ghassemlooy, "Channel characterization for indoor visible light communications," in *Proc. 3rd Int. Workshop Opt. Wireless Commun. (IWOW)*, Funchal, Portugal, Sep. 2014, pp. 75–79.
[36] A. Nuwanpriya, S.-W. Ho, and C. S. Chen, "Angle diversity receiver for indoor MIMO visible light communications," in *Proc. IEEE Globecom Workshops (GC Wkshps)*, Austin, TX, USA, Dec. 2014, pp. 444–449.

Rui Wang (M'14) received the B.S. degree from Anhui Normal University, Wuhu, China, in 2006, the M.S. degree from Shanghai University, Shanghai, China, in 2009, and the Ph.D. degree from Shanghai Jiao Tong University, China, in 2013, all in electronic engineering. From 2012 to 2013, he was a Visiting Ph.D. Student with the Department of Electrical Engineering, University of California at Riverside, Riverside, CA, USA. From 2013 to 2014, he was with the Institute of Network Coding, The Chinese University of Hong Kong, as a Post-Doctoral Research Associate. From 2014 to 2016, he was an Assistant Professor with the College of Electronics and Information Engineering, Tongji University, where he is currently an Associate Professor. His current research interests include wireless cooperative communications, MIMO technique, network coding, and OFDM.

Qian Gao received the bachelor's degree (Hons.) from the Nanjing University of Science and Technology in 2009, and the M.Sc. and Ph.D. degrees from the University of California at Riverside, Riverside, CA, USA, in 2010 and 2014, respectively (Deans Distinguished Fellowship), all in electrical engineering. He has been with the Center of Ubiquitous Communications by Light and interned with the United Nations Headquarters, New York, NY, USA. He is currently on the faculty with the University of Science and Technology of China. His current research interests include optical wireless communications, big data analytics and wireless full-duplex radio. He has contributed multiple standardization documents to the IEEE 802.15 on visible light communications. He has served as a TPC member for international conferences and was recognized as a Top Reviewer for Optical Engineering (SPIE). He is currently an Associate Editor of the *EURASIP Journal on Wireless Communications and Networking* and a Grant Reviewer for the NSFC and the OSA.

Jiayi You received the B.E. degree in communication engineering from East China Normal University, China, in 2015. She is currently pursuing the master's degree with the College of Electronics and Information Engineering, Tongji University. Her current research interests include wireless cooperative communications, MIMO technique, and indoor positioning.

Erwu Liu (SM'11) received the Ph.D. degree from the State Key Laboratory, Huazhong University of Science and Technology, in 2001. From 2001 to 2007, he served Alcatel-Lucent as a Project Manager, Senior Consultant, and Senior Research Scientist. From 2007 to 2011, he was with the Imperial College London, as a Research Associate. Since 2011, he has been a Professor with Tongji University. His current research interests include complex network and big data, Internet of Things, wireless sensor networks, deep-penetration communications, indoor localization, and 5G technologies. He is currently a fellow of the IET, ALTA member of Alcatel-Lucent Technical Academy, and senior member of ACM. He has developed the first through-the-earth communication device in China, and won the Championship of Microsoft Indoor Localization Competition (IPSN) 2016, the Silver Innovation Award in China Industry Industry Fair (CIIF) 2016, and the Grand Prize Award in CIIF 2014. He serves as an Editor for various journals, such as the IEEE COMMUNICATIONS LETTERS, the *KSII Transactions on Internet and Information and Systems*, and *China Communications*.

Ping Wang received the Ph.D. degree from the Department of Computer Science and Engineering, Shanghai Jiaotong University, in 2007. He is an Associate Professor with the Department of Information and Communication Engineering, Tongji University. His current research interests include routing algorithms and resource allocation of wireless networks (especially for VANETs). He is responsible for constructing the testing field of cellular-based broadband vehicular communication technologies in Shanghai auto city.

Zhengyuan Xu received the B.S. and M.S. degrees from Tsinghua University, China, and the Ph.D. degree from the Stevens Institute of Technology, USA. He was with the University of California at Riverside, Riverside, CA, USA, from 1999 to 2010, where he became a Full Professor with tenure and also a Founding Director of the Center of Ubiquitous Communications by Light. In 2010, he was selected by the Thousand Talents Program of China and appointed as a Professor with Tsinghua University. Since 2013, he has been a Professor with the Department of Electronic Engineering and Information Science, School of Information Science and Technology, University of Science and Technology of China (USTC). He is the Founding Director of Wireless-Optical Communications Key Laboratory with the Chinese Academy of Sciences, the Founding Director of Optical Wireless Communication and Network Center with USTC, and a Chief Scientist with the National Key Basic Research Program of China. He has authored over 270 journal and conference papers. His research focuses on wireless communication and networking, wireless big data, optical wireless communications, geolocation, and signal processing. He was an Associate Editor and a Guest Editor for various IEEE journals, and the Founding Co-Chair of the IEEE GLOBECOM Workshop on Optical Wireless Communications in 2010. He has delivered tutorials, keynote speeches, and invited talks on optical wireless communications in various international conferences.

Yingbo Hua (S'86–M'88–SM'92–F'02) received the B.S. degree from Southeast University (formerly known as Nanjing Institute of Technology), Nanjing, China, in 1982, and the Ph.D. degree from Syracuse University, Syracuse, NY, USA, in 1988. He was on the faculty of The University of Melbourne, Melbourne, VIC, Australia, from 1990 to 2000, where he was promoted to the rank of Reader and Associate Professor in 1995. Following a sabbatical leave as a Visiting Professor with the Hong Kong University of Science and Technology from 1999 to 2000, and as a Consultant with Microsoft Research, WA, USA, in summer 2000, he joined the University of California at Riverside, Riverside, CA, USA, in 2001, where he is a Senior Full Professor. He has authored extensively in the fields of signal processing, wireless communications, and sensor networks, including such topics as high resolution methods, sensor array processing, blind source separation, blind system identification, reduced rank estimation, principal component analysis, subspace tracking, MIMO relay beamforming, MIMO channel estimation, multi-hop networks, full-duplex radio, resource allocation, and physical layer security.

Dr. Hua is a fellow of AAAS from 2011. He has served on the Editorial Boards for several top journals in his research fields. He is currently a Senior Area Editor of the IEEE TRANSACTIONS ON SIGNAL PROCESSING and a Steering Committee Member of the IEEE WIRELESS COMMUNICATIONS LETTERS.